



Taking Nanotechnological Remediation Processes from Lab Scale to End User Applications for the Restoration of a Clean Environment

Project Nr.: 309517

EU, 7th FP, NMP.2012.1.2

WP 6: Analytical Methods for *In-situ* Determination of Nanoparticles Fate.

DL 6.1 Feasibility and Applicability of Monitoring Methods

Deborah Oughton (NMBU), Melanie Auffan (CERGE),
Steffen Bleyl (UFZ), Julian Bosch (HMGU), Jan Filip (UPOL),
Norbert Klaas (USTUTT), Jonathan Lloyd (UMAN),
Frank van der Kammer (UNIVIE).

March 31st 2015



[Downloaded from www.nanorem.eu/toolbox](http://www.nanorem.eu/toolbox)

The research leading to these results has received funding from the
European Union Seventh Framework Programme (FP7/2007-2013)
under Grant Agreement n° 309517

List of co-authors:

Name, First Name	Partner Organisation	
Hans-Christian Teien, Ole Christian Lind, Merethe Kleiven	Norwegian University of Life Sciences	
Stephan Wagner, Doris Schmid, Andreas Gondikas, Milica Velimirovic	University of Vienna	
Norbert Klaas	University of Stuttgart, VEGAS	
Anett Georgi, Glenn Gillies, Katrin Mackenzie, Steffen Bleyl	UFZ	
Jonathan Lloyd, Vicky Coker, Mat Watts, James Byrne, Richard Patrick, Nimisha Joshi	University of Manchester	
Julian Bosch	Helmholtz Zentrum München	
Jan Filip	Palacky University Olomouc	
Melanie Auffan, Armand Maison	Centre National de la recherche scientifique	

Reviewed by PAG member(s):

Name, First Name	Partner Organisation
Gerhardt, Rolf	Deutsche Bahn AG
Lowry, Greg	Carnegie Mellon University
Matz, Pierre	Solvay

Table of Contents

1	Content and aim of the deliverable	1
2	Characterisation requirements as a function of the remediation phase and method type	2
2.1	<i>Remediation Phases.....</i>	2
2.1.1	Pre-injection Phase	2
2.1.2	NP Injection Phase	3
2.1.3	System Recovering Phase	3
2.1.4	Long Term Steady State Phase (monitoring of success)	3
2.2	<i>Type of Characterisation Method</i>	3
3	Laboratory Methods	4
3.1	<i>Particle sizes, dispersion and concentration</i>	4
3.1.1	Dynamic Light Scattering (DLS) and Laser Diffraction.....	5
3.1.2	Time of Transition Measurement	5
3.1.3	Sedimentation Rate	6
3.1.1	Turbidity.....	7
3.1.2	Sedimentation Field flow Fractionation (SedFFF).....	8
3.1.3	Electron Microscopy (TEM, SEM).....	8
3.1.4	Electroacoustics	8
3.2	<i>General chemical analysis (Fe-concentration, pH, conductivity, etc.).....</i>	9
3.3	<i>Particle structure.....</i>	9
3.3.1	X-ray magnetic circular dichroism (XMCD)	9
3.3.2	X-ray absorption near edge and extended fine structure spectroscopy; XAFS and XANES Cr K-edge spectroscopy	10
3.4	<i>Radiolabelling</i>	11
3.4.1	Neutron Activation	12
3.4.2	Tc-99m	12
3.5	<i>Micro Tomography (MicroXCT).....</i>	13
4	<i>In situ measurement</i>	13
4.1	<i>Magnetic susceptibility</i>	13
4.2	<i>Temperature and redox</i>	14
4.3	<i>H₂ production</i>	15
5	On site sampling and measurement	16
5.1	<i>Size fractionation/ultrafiltration.....</i>	16
5.2	<i>Turbidity.....</i>	17
5.3	<i>Fe content and conductivity.....</i>	18
5.4	<i>Mossbauer: nZVI</i>	19
5.5	<i>H₂ Production: Acid Digestions</i>	20
5.6	<i>X-ray powder diffraction: nZVI.....</i>	21
5.7	<i>ICP-MS and rare earth elements.....</i>	22
6	Carbolron and Fe zeolites.....	23
6.1	<i>Carbolron: Fe/C ratios.....</i>	23
6.2	<i>Carbolron: Temperature Programmed Oxidation (TPO).....</i>	23
6.3	<i>Fe-Zeolites.....</i>	25
7	Summary: Applicability of the Methods	28
8	List of References.....	31

List of Figures

Figure 1: Left: correlation between turbidity and particle concentration (expressed as TSS in g/L) in standard EPA water (according to DL4.1 F.I.m); Right: particle suspension extracted during the VEGAS tank experiment. .8	8
Figure 2: XMCD analysis of biomagnetite during scale-up in reaction volumes of 10 ml, 100 ml , 1 L and 10 L (Byrne et al., in revision). (a) “Bio mag” corresponds to sample of biogenic magnetite with close to stoichiometric cation distribution. (b) X-ray magnetic circular dichroism (XMCD) derived from difference between two XAS collected with sample under influence of a magnetic field of + and – 0.6 T respectively.....10	10
Figure 3: XAFS profiles of oxidation state standards of Fe compounds compared with the profile of a bulk nano Fe star sample. The measurements were performed at the BM26 - DUBBLE - Dutch-Belgian Beamline, ESRF (Nuyts et al, unpublished results). 11	11
Figure 4: XANES analysis of Cr during remediation (Watts et al 2015).....11	11
Figure 5: Radiolabelling with Tc-99m.....12	12
Figure 6: MicroXCT of optimized NF particles in a column of sand during mobility experiment and its grey scale histogram. The sand is in grey, the pores are in blue, and the iron is in yellow. FOV: Field of view. The red area on the histogram represents the iron thresholding.....13	13
Figure 7: Susceptibility probe, electromagnetic field (left), position and shape of the inductors (right).....14	14
Figure 8: Sensor-arrays before installation in the aquifer.14	14
Figure 9: Variation in size distribution of Fe at position 3eD (ca 1 m from injection) in the Vegas tank with increasing time after injection of FeOx NP. Fe concentrations determined by ICP-OES (Perkin Elmer Optima 5300 DV).Analysis of the 0,45 um and 10 kDa fractions hr is ongoing.17	17
Figure 10: Turbidity data indicating particle distribution at different depths (Level 2-6) 20 hours after injection of FeOx at the VEGAS Tank Experiment.....17	17
Figure 11: Iron total and electrical conductivity measured in the four monitoring wells around the injection well over 3 depth layers (level2 – level4) and over the timeframe of the FeOx nanoparticle injection at the VEGAS tank experiment.....18	18
Figure 12: Room-temperature Mössbauer spectrum of a sample collected from Spolchemie, PV-130, 10.12.2014.20	20
Figure 13: XRD pattern of the sample PV_130_20141012 collected from Spolchemie, PV-130, 10.12.2014.21	21
Figure 14: ICP-MS determination of the concentration in ng/L of selected elements in 5 different batches of nZVI iron nanoparticles.22	22
Figure 15: The ratio $c_{Fe,total}/c_{POC}$ at CMT measuring points (with depth profile) at a site in Celle/Bergen.23	23
Figure 16: Temperature-programmed oxidation (TPO) of carbonaceous materials in a thermos-gravimetric balance (TGA-50 Shimadzu: air flow rate 50 mL/min; $m_{sample} = 6...16$ mg; $\Delta T: 10$ K/min; $T_{max} = 700^{\circ}C$).....24	24
Figure 17: Calibration curves for determination of the concentration of Fe-BEA-35 in aqueous suspension by means of measurement of absorbance at 860 nm (UV-Vis instrument Varian Cary 300) (right figure for concentration range 0.1 – 2.5 g/L).....26	26
Figure 18: Calibration curve for determination of Fe-BEA-35 on Ottawa quartz sand by BET analysis.....26	26
Figure 19: Calibration function for indirect determination of zeolite weight fraction (Fe-BEA-35) in sand (M.I) via adsorption of MTBE (c_{total}/c_e = concentration of total MTBE added / equilibrium aqueous phase concentration)27	27
Figure 20: UV-Vis spectrum in diffuse reflectance mode for fluorescent zeolite (FLU-BEA-35); its fluorescence spectrum ($\lambda_{ex} = 385$ nm, suspension in deionized water) and photo of suspensions under daylight (photo left) and UV light (photo right) (left figure); Calibration data for fluorescence detection of FLU-BEA-35 in deionized water (right figure).....28	28

List of Tables

Table 2.1: Summary of Nanoparticle Characterisation Methods	4
Table 3.1: Performance of Zetasizer for Nanoparticle DLS Characterisation	5
Table 3.2: Performance of Mastersizer for Nanoparticle Characterisation	5
Table 3.3: Performance of Eyetech for Nanoparticle Characterisation	6
Table 3.4: Performance of Turbiscan for Nanoparticle Characterisation	7
Table 3.5: Activation products and half-lives (Nanofer STAR)	12
Table 4.1: Hydrogen gas measurement- 'A' refers to the surface of the wellhead and for 'B' the exact point of the measurement was inside the well, above the water level.	15
Table 5.1 Size distribution of Fe in FeOx stock solutions: hollow-fibre ultrafiltration.....	16
Table 7.1: Summary of Applicability of Selected Nanoparticle Characterisation Methods.....	29

1 Content and aim of the deliverable

All remediation applications need to document the effectiveness of the technologies. A major challenge in following the fate of engineered nanoparticles is their detection in environmental media, and in particular their isolation from background metal and natural colloidal material. This represents a particular hurdle for the use of Fe-based NPs in remediation, owing to high levels of naturally occurring iron. The overall goal of WP6 is the development and application of analytical methods and protocols for in-situ measurement and detection of nanoparticles. Within WP6 the work is divided into three main areas:

1. Optimisation of monitoring and tracing tools. To optimize techniques based on measurement of the ferro-magnetic properties (susceptibility) of iron for monitoring iron NPs in the field. To determine the feasibility and applicability of isotope and trace metal techniques for laboratory and field applications.
2. Application of modern high performance analytics. To develop protocols for on-site measurements and in-situ characterization of natural and engineered nanoparticles. To develop methods for detection of Carbo-Iron and Fe-zeolites.
3. Laboratory and field tests of the methods. To consolidate the available methods, evaluate their applicability for Fe-based and in-situ application and review the analytical capacities of partners. To provide documentation of “fit for purpose”, detection limits and costs, and assessments of the potential for routine application.

This deliverable report presents the first summary of the feasibility and applicability of a variety of methods that could be applied for NP characterization. The work is primarily based on testing of the methods in laboratory studies, but also includes initial results from the large-scale tank studies carried out with FeOx in VEGAS in October 2014, as well as the on site application of nZVI and FeOx at Usti/Spolchemie in November 2014. The report focuses on the potential applicability of the methods. It does not carry out an assessment of the mobility and performance of the NPs in the laboratory or field experiments. That will be reported in separate WP deliverables. The final deliverable report D6.2 “Analytical Toolbox for in-situ and on-site Monitoring” is due in month 44 and will consolidate experience and recommendations for analytical methods.

Whilst the overall WP objective aims at the applicability *in situ* (i.e. within the field), a good deal of experience is available from application in laboratory studies, and particularly those to study the mobility and fate of nanoparticles (NP) in various test media. However, laboratory experiments tend to use rather high concentrations of nanoparticles (NP), in simple media, and can rely on relatively straightforward methods for NP measurement and characterization. Measurement during field applications is more challenging due to more complex and heterogeneous media and different requirements for information during the different stages of remediation. Thus, the present report covers the applicability of methods for Fe-based NPs, as well as specific challenges, advantages and factors influencing detection limits for field measurements.

The applicability of the methods also depends on the phase of remediation and the question to be addressed. As for any *in situ* remediation technologies, an assessment will need to be made of the success of the method and temporal and spatial variation in efficiency. The different phases are de-

scribed in more detail in the next section. But, briefly, for field applications the requirements can be divided into four main areas, all having different analytical requirements and issues.

- (1) Field characterisation studies prior to injection
- (2) Monitoring the movement and distribution of particles during injection. Is the particle suspension reaching the required location, with the required concentration and state? While the NP concentrations are relatively high, there is a need for rapid feedback at relatively high resolution.
- (3) Monitoring for transport of “fine” or “renegade” out of the core application area during and after injection. Low NP concentrations give rise to challenges with detection against background levels of colloids. But monitoring can be carried out with a lower spatial resolution, and less urgency for a rapid feedback.
- (4) Post injection behaviour. Transformation and reactivity of the particles. Need for reinjection.

The methods can also be distinguished into general laboratory methods for characterization, “truly” *in situ* measurements that actually monitor particles within the aquifer and methods that combine *in situ* or at site sampling with subsequent at site or laboratory measurement. The following section gives a general overview of the different requirements for NP characterisation as a function of remediation phase. Sections 3-5 of the report describes the various methods, focusing primarily on methods where tests have been initiated at the tank and field sites. Section 6 gives an update on method development for Carbolron and Fe-zeolites. Section 7 summarises the methods according to strengths and limitations and detection limits.

2 Characterisation requirements as a function of the remediation phase and method type

2.1 Remediation Phases

During the application of a remediation technology a number of analytical and monitoring techniques will need to be employed, and the different phases will have specific requirements concerning the analytical techniques. While the present report only deals with nanoparticle characterisation methods, it is important to consider how these relate to the other analysis and monitoring requirements, and more importantly how these change with remediation phase. This holds true for field application as well as for laboratory studies with slightly different needs for the two. These phases are described in the next sections together with their special properties and requirements regarding the overall monitoring strategies and systems.

2.1.1 Pre-injection Phase

The measurement techniques applied in this phase are mostly standard methods used in chemical or hydraulic engineering. Measurement systems such as sampling and injection wells, or in-situ sensors (if needed) have to be installed, and disturbances of the system need to be accounted for, depending on the ground water velocity and the time expected for stabilizing of the system. The main task for is to describe the temporal and spatial concentration profiles of contaminants, but sampling can also provide background and baseline data of relevance for NP tracking.

2.1.2 NP Injection Phase

The requirements in this phase are very different from the previous and also from the following phases. The main focus is the behaviour of the particles, namely the radius of influence (ROI), the travel distance and the homogeneity of the distribution around an injection point of well, and acute changes within minutes have to be detected. This requires not only much higher measurements frequencies, but also the application of different measurement techniques.

Since particles are injected as a suspension, the liquid and the solid phases may behave differently, and methods need to address both phases in order to provide information about the overall efficiency of the injection and potential deviations from the planned behaviour. For the liquid phase relatively simple methods are available such as temperature measurements (usually the temperature of the injected fluid differs from the ground water temperature) or the addition of tracer substances (dyes or tracer ions) to the suspension. For the particles, unfortunately, only a few in-situ methods are available. Thus, in most cases the particle detection will have to be based on sampling and on-site or laboratory methods (see section 3-4 below). This phase has a duration of hours to days.

2.1.3 System Recovering Phase

This phase is the intermediate phase between the injection with a considerable disturbance of the hydraulic system in the aquifer and the tranquillisation back to the natural ground water flow and the removal of the injected fluid by the ground water. During this phase intensive analytical activities for both particles and contaminants are usually not reasonable, because the dissolved compounds are in a transient state. This means that during the recovery phase a reduced monitoring program is advisable where only some main chemical parameters are monitored, in order to determine the point in time where the natural conditions have re-established (natural conditions taking into account the modifications to be expected by the injected particles).

2.1.4 Long Term Steady State Phase (monitoring of success)

During this phase an intensive monitoring is carried out, in order to verify the success of the remediation. In addition to monitoring of particles, the monitoring program would include the contaminants, reaction products, metabolites and general milieu parameters of the ground water. The main focus of the monitoring is to ensure the efficiency of the desired reaction and the point in time when the activity of the particle ceases. The criteria for the decision about a success of an application of particles have to be fixed beforehand and a monitoring program chosen accordingly. All the findings of the monitoring will be compared to the status defined during the characterisation phase (see 2.1.1).

2.2 Type of Characterisation Method

This deliverable focuses on methods that are relevant for the characterization of Fe-based nanoparticles. Methods include standard nanoparticle characterisation methods (e.g., DLS, EM), as well as specific methods for Fe-based nanoparticles developed for remediation purposes. A summary of the various methods is given in Table 2.1, divided into laboratory characterisation methods, in site measurements and on site applications, and each are described in more detail in the following three sections. Aspects covered include applicability for on site or *in situ* measurements linked to remediation,

as well as issues of relevance for the analysis of Fe-based nanoparticles. Advantages and limitations, and where possible detection levels and/or factors impacting on detection levels are included. Further practical details on the methods available from different NanoRem partners (instrumentation details, contact names, etc.) can be found in IDL 6.1: the analytical toolbox database.

Table 2.1: Summary of Nanoparticle Characterisation Methods

Type of Method	Examples	Applications	Comments
Laboratory Particle characterisation	Acid digestion, FFF, ICP-MS, TEM, DLS, synchrotron techniques, isotope and rare earth metal methods etc.	All particle characteristics: size, structure, composition, aggregation, mineralogy etc.	Required to understand fundamental particle behaviour in laboratory and field experiments
In-situ measurement and characterisation	Ferro-magnetic methods; redox measurement; H ₂ production	Particle concentration, particle reactivity	Possibility for high data resolution over time and space
On site application: sampling and measurement techniques	Turbidity, Fe spectrometry, ultrafiltration; stable isotope and rare earth ratios; Mössbauer	Particle size, Zeta potential, and particle concentration, Fe concentration	Sampling can also be combined with further laboratory analysis (including isotope techniques) to provide more detailed information on field behaviour, and/or particle reactivity

3 Laboratory Methods

This section concentrates on the applicability of various standard nanoparticle characterisation and tracing techniques to the analysis of Fe based NPs. They include routine particle size and concentration measurements such as DLS and EM, general chemical analysis and radiolabelling techniques. Many challenges for the methods are similar to those for other NPs, such as the stability of the suspensions (e.g. problems with aggregation and sedimentation) as well as the specific impact of redox on Fe speciation (e.g., precipitation of dissolved Fe going from anoxic to oxic conditions)

3.1 Particle sizes, dispersion and concentration

A number of different techniques are routinely applied for particle characterization. This section gives a brief overview of the applicability and performance of such techniques to NanoRem nanoparticle

3.1.1 Dynamic Light Scattering (DLS) and Laser Diffraction

Zetasizer (Malvern, ZetaSizer Nano): The DLS technique measures diffusion of the particles and calculate the particles hydrodynamic radius from 1 nm up to about a micrometer using dynamic light scattering. The method can be used to determine particle concentrations in clean solutions, provided that the suspensions are below 500 mg L⁻¹ particle concentration, and particles less than 1 µm. Fast sedimentation makes the size analysis impossible for larger particles (> 1 µm).

Table 3.1: Performance of Zetasizer for Nanoparticle DLS Characterisation

Particles (producer)	Method	Limitation
Nanofer products (Nanofer 25S, Nanofer Star, Modified Nanofer Star) (Nanoiron)	measured concentration 200 mg L ⁻¹ (1g L ⁻¹ diluted 1:5)	Fast sedimentation of the particles
Milled Iron (UVR-FIA)	measured concentration 200 mg L ⁻¹ (1g L ⁻¹ diluted 1:5)	Size above limit of detection Fast sedimentation of the particles
Carbo Iron (UFZ)	measured concentration 200 mg L ⁻¹ (1g L ⁻¹ diluted 1:5)	
Fe-Zeolites (UFZ)	measured concentration 200 mg L ⁻¹ (1g L ⁻¹ diluted 1:5)	
Bio-Fe-oxides (UMAN)	measured concentration 200 mg L ⁻¹ (1g L ⁻¹ diluted 1:5)	High size variation due to different batches
Fe-oxides (HG MU)	measured concentration 200 mg L ⁻¹ (1g L ⁻¹ diluted 1:5)	

Mastersizer (Malvern, Mastersizer 2000): The method is based on determination of the volume equivalent spherical diameter based on laser light diffraction (small angle light scattering). Mie theory is used to calculate particle size distributions from scattering patterns of two different light sources (red and blue laser). Small angle scattering is used for particles > 1 µm and wide angle scattering is used for particles < 1 µm. The main limitations are that high concentration (> 500 mg L⁻¹) and larger sample volume (>=15 mL) are required.

3.1.2 Time of Transition Measurement

Eyeteck: Eyeteck using the laser obscuration with the time of transition measurement principle gives information on the particle number based distribution of the geometric radius of the particles. The method can be applied to a particle size range of 0.6 up to 600 µm, and can measure concentrations well below 500 mg L⁻¹. As for DLS, fast sedimentation of larger particles is a challenge, although for nZVI particles a mechanical stirrer was used to prevent particles from sedimentation. The Eyeteck-System also enables both the concentration and the particle shape to be estimated.

Table 3.2: Performance of Mastersizer for Nanoparticle Characterisation

Particles (producer)	Method/ Limitations
Nanofer products (Nanofer 25S, Nanofer Star, Modified Nanofer Star) (Nanoiron)	Refractive index: 2.87 Absorption: 3.35
Milled Iron (UVR-FIA)	Refractive index: 2.87 Absorption: 3.35
Carbo Iron (UFZ)	Refractive index: 2.87 Absorption: 3.35
Fe-Zeolites (UFZ)	Refractive index:1.59 Absorption: 0.01
Bio-Fe-oxides (UMAN)	Refractive index:2.42 Absorption: 0.1 Low sample value for analyses
Fe-oxides (HGMU)	Refractive index:1.8 Absorption: 0.1 Particle size below limit of detection (<300 nm)

Table 3.3: Performance of Eyetech for Nanoparticle Characterisation

Particles (producer)		Limitation
Nanofer products (Nanofer 25S, Nanofer Star, Modified Nanofer Star) (Nanoiron)	measured concentration 200 mg L ⁻¹ (1 g L ⁻¹ diluted 1:5)	Fast sedimentation of the particles
Milled Iron (UVR-FIA)	measured concentration 200 mg L ⁻¹ (1 g L ⁻¹ diluted 1:5)	Fast sedimentation of the particles
Carbo Iron (UFZ)	measured concentration 200 mg L ⁻¹ (1 g L ⁻¹ diluted 1:5)	
Fe-Zeolites (UFZ)	measured concentration 200 mg L ⁻¹ (1 g L ⁻¹ diluted 1:5)	
Bio-Fe-oxides (UMAN)	measured concentration 200 mg L ⁻¹ (1 g L ⁻¹ diluted 1:5)	High size variation due to different batches
Fe-oxides (HGMU)	measured concentration 200 mg L ⁻¹ (1 g L ⁻¹ diluted 1:5)	Below limit of detection (<600 nm)

3.1.3 Sedimentation Rate

TurbiScan LAB EXPERT: Phase separation in a particle dispersion is continuously determined by vertically scanning the measurement vial for light absorption and scattering. Using the sedimentation rate the particle size (hydrodynamic radius) can be calculated via Stoke's equation. 20 ml of particle sus-

pension are used and sedimentation rate is measured at stable temperature over a specified time interval.

$$R_H = a = \frac{k_b T}{6\pi\eta D}$$

Stoke's law, where k_b is the Boltzmann constant, T is the temperature, η is the liquid's viscosity, and D is the diffusion coefficient.

Table 3.4: Performance of Turbiscan for Nanoparticle Characterisation

Particles (producer)	Measurement time	Limitation
Nanofer products (Nanofer 25S, Nanofer Star, Modified Nanofer Star) (Nanoiron)	25 min	Some particles stick to the measurement cell surfaces
Milled Iron (UVR-FIA)	25 min (for unstabilized milled Iron particles)	
Carbo Iron (UFZ)	60 min (for CMC stabilized particles)	
Fe-Zeolites (UFZ)	60 min (for CMC stabilized particles)	
Bio-Fe-oxides (UMAN)	25 min	High size variation due to different batches
Fe-oxides (HGMU)	>12 hours (depending on concentration)	

3.1.1 Turbidity

An increase in particle concentration results in an increase in the turbidity of the sample. This simple relation can be used to estimate the particle concentration in water samples. The turbidity parameter [expressed as NTU] for different particle concentrations (g/L) was determined in laboratory tests using different water qualities. The correlation between NTU and particle concentration depends on the water quality. Therefore, to obtain reproducible results calibration of the turbidity and particle concentration calculation has to consider the water quality. An example for the calibration is given in Figure 1. The used instrumentation allowed us to estimate particle concentrations up to 1 g/L. Above 1 g/L a reliable estimate for particle concentration could be obtained by dilution.

The turbidity parameter was used to estimate particle concentration in the effluent from column experiments and Fe-content was inferred from the results.

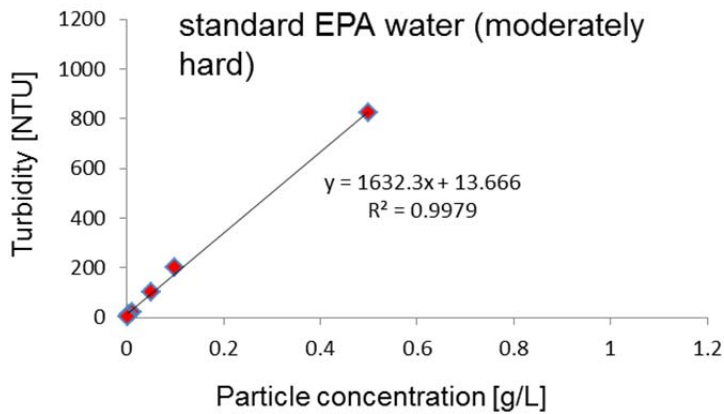


Figure 1: Left: correlation between turbidity and particle concentration (expressed as TSS in g/L) in standard EPA water (according to DL4.1 F.I.m); Right: particle suspension extracted during the VEGAS tank experiment.

3.1.2 Sedimentation Field flow Fractionation (SedFFF)

UNVIE will develop a sedimentation field flow fractionation (SedFFF) based method for the characterization of iron-bearing nanoparticles. SedFFF separates particles based on differences in size and density and therefore has high applicability for complex samples which contain particles of varying origin, such as natural samples. The goal is to utilize a combination of detectors (e.g. UV, static and dynamic light scattering, elemental concentrations with ICPMS) on-line with the SedFFF, with parallel collection of fractions that can be used for particle specific analysis (e.g. single particle ICPMS and electron microscopy). In addition, an option will be given to perform the analysis in anaerobic conditions, in order to avoid changes in particle size and density caused by oxidation and the formation of new iron phases during the analysis. Once developed, this setup will offer very powerful characterization capabilities. Currently the operation parameters of the SedFFF are being optimized.

3.1.3 Electron Microscopy (TEM, SEM)

Electron microscopy has been applied for the characterisation of all NanoRem NPs, and is part of the standard information provided on stock particles (see WP2 and WP3). TEM has been used for characterisation of NP size and size distribution in laboratory and field studies, including characterisation of ecotox exposure solutions (See DL5.1), and has the advantage of being able to cope with a wide range of size and concentrations. Limitations are similar to those for other NPs, such as aggregation during sample preparation.

3.1.4 Electroacoustics

The use of electro acoustic methods for the characterisation of suspensions is a relatively new method (www.Quantachrome.de), and is currently under development by USTUTT. By sonification of suspensions or emulsions with different frequencies of ultrasound, various parameters can be deduced such as:

- viscosity,
- particle size, particle size distribution and
- zeta potential.

The method is complementary to light scattering techniques, since it can be used for highly concentrated suspensions or emulsions without dilution (particle concentrations between 1% and > 50%). For the application of particles for remediation purposes this method is extremely powerful, because the suspension can be stirred during the measurement and the surface charge of the particles can be deduced from the raw data. This gives a good understanding of the real cause for the mobility of the particles under the conditions of an injection.

3.2 General chemical analysis (Fe-concentration, pH, conductivity, etc.)

The standard chemical methods used to study mobility of particles under laboratory conditions can also be applied to monitor the behaviour of NP in the field. Changes in Fe concentration, pH, temperature, and conductivity can provide a relatively rapid assessment of the spatial and temporal status of the particle distribution in the liquid phase. The total particle loading can be measured by gravimetric measurements (drying and weighing) and even colour changes can give a rapid qualitative assessment. For total Fe concentration, measurements on suspensions/liquids and soils/sediments can either be carried out after acid digestion and measurement using standard chemical analysis (e.g., ICP-OES, or spectrophotometry). For low particle densities, pre-concentration by centrifugation or filtration can be applied to improve detection limits. Specific protocols for acid digestion need to be developed for the different particles to ensure complete dissolution (Braunschweig et al., 2012). The detection limits of all methods will be site specific, depending largely on the background levels, and, for Fe-based NPs, dissolved iron concentrations. More information on site applicability can be found in Section 5.3.

3.3 Particle structure

A wide range of synchrotron-based techniques have been developed and assessed for the analysis of Fe-based nanomaterials. Examples given below include applications to studies of the scalable production of bionanomagnetite, and the treatment of contaminants including Cr(VI) in NanoRem (UMAN) and NanoferSTAR stability (NMBU). While the methods are not expected to be routine applications in field monitoring, they have been applied in laboratory studies, and do have powerful potential to shed light on potential changes in speciation and structure of particles under field conditions.

3.3.1 X-ray magnetic circular dichroism (XMCD)

XMCD is a synchrotron technique used to determine oxidation states and extended crystal structure of magnetic nanomaterials. This powerful technique has been applied to the study of biomagnetite synthesis, confirming that the structure of the biomineral is conserved during scale-up from 10 ml bottles to a 10L bioreactor. X-ray absorption spectra (XAS) of samples obtained through Fe(III) reduction are shown in Fig 2. Spectra display peaks corresponding to Fe²⁺[B], Fe³⁺(A) and Fe³⁺[B] as highlighted by fits blue, red and green respectively..

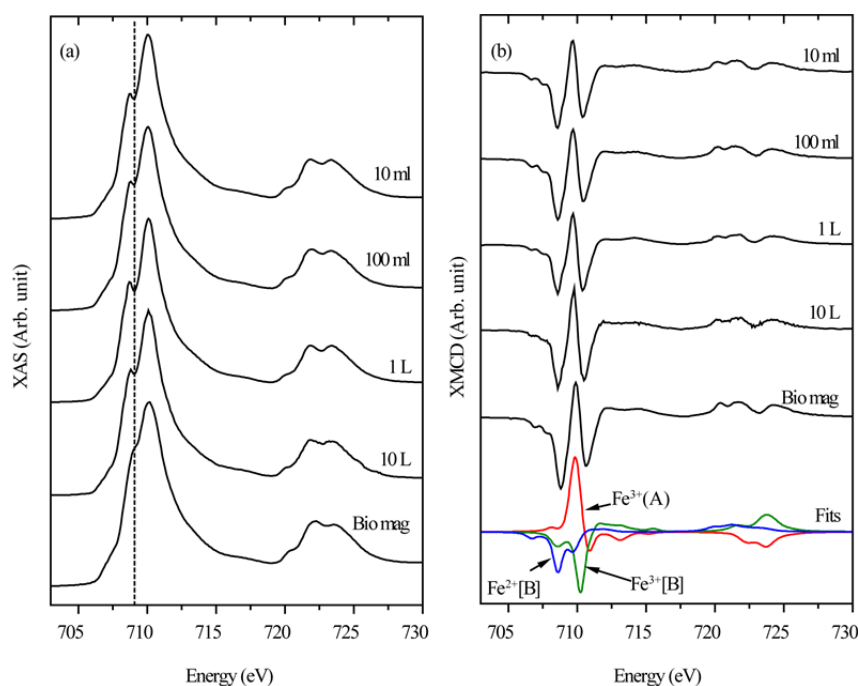


Figure 2: XMCD analysis of biomagnetite during scale-up in reaction volumes of 10 ml, 100 ml, 1 L and 10 L (Byrne et al., in revision). (a) “Bio mag” corresponds to sample of biogenic magnetite with close to stoichiometric cation distribution. (b) X-ray magnetic circular dichroism (XMCD) derived from difference between two XAS collected with sample under influence of a magnetic field of + and – 0.6 T respectively.

3.3.2 X-ray absorption near edge and extended fine structure spectroscopy; XAFS and XANES Cr K-edge spectroscopy

XAS analyses have also been used to study the NP structure (Fig. 3) as well as contaminant fate (e.g. for Cr during NanoRem experiments). Chromite ore processing residues form significant source of Cr(VI) contamination globally. Leachate samples were collected from a field site in Glasgow, UK. Here the significant pool of soluble Cr(VI) minerals (~10000 mg/Kg) have created a hyperalkaline high Cr(VI) (> 1mM) leachate. Biomagnetite was able to source stabilise the readily leachable Cr(VI) by reduction to Cr(III) and reduce a significant fraction of mineral bound Cr(VI) with modest additions of biomagnetite (5% w/w) and NANO FER 25S (2% w/w). It was also found recalcitrant to air re-oxidation. Cr oxidation state in sediment microcosms was identified by XANES (Fig. 4).

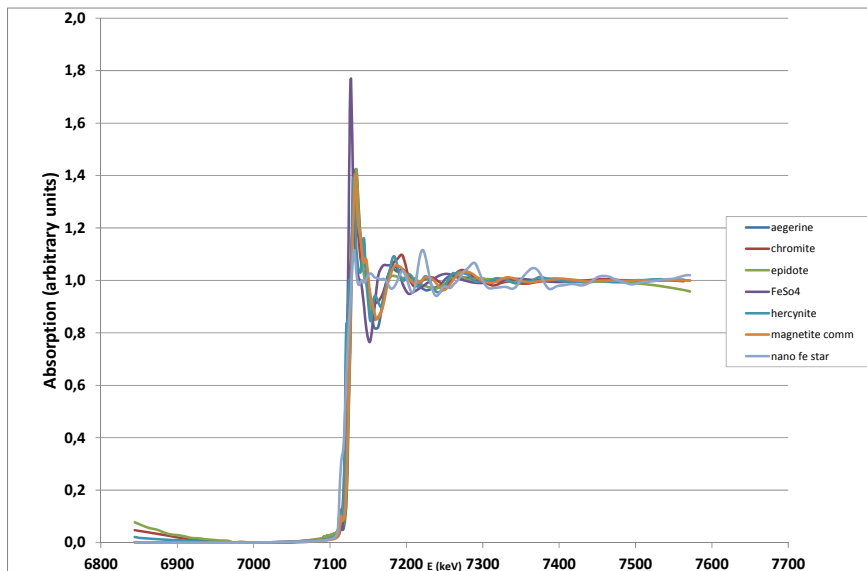


Figure 3: XAFS profiles of oxidation state standards of Fe compounds compared with the profile of a bulk nano Fe star sample. The measurements were performed at the BM26 - DUBBLE - Dutch-Belgian Beamline, ESRF (Nuyts et al, unpublished results).

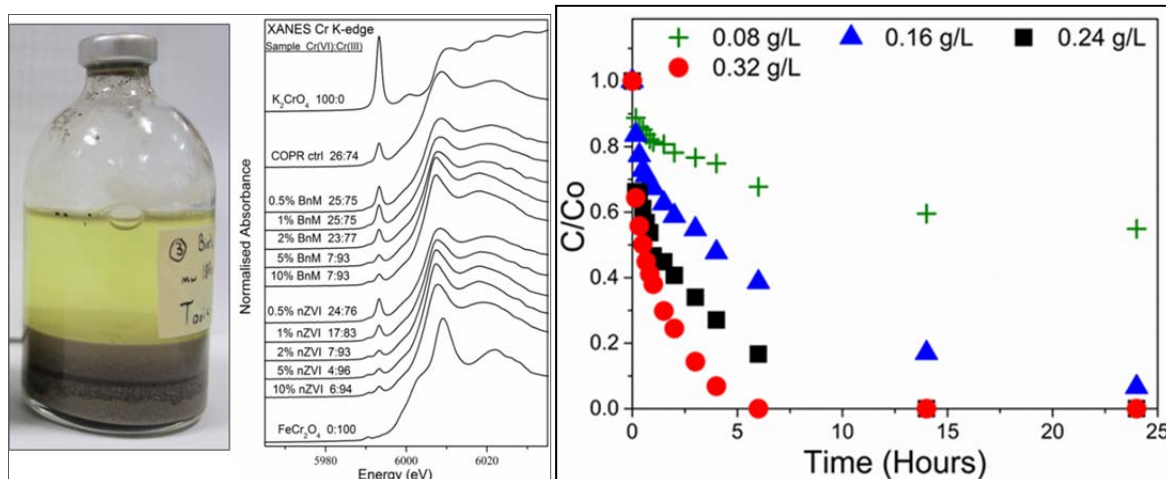


Figure 4: XANES analysis of Cr during remediation (Watts et al 2015).

3.4 Radiolabelling

Radiolabelling of nanoparticles has a high potential for detection of very low concentrations of NPs, also in cases where interference from background matrices can be high. Three main radiolabelling techniques have been developed within NanoRem: neutron activation of powders, labelling with Tc-99m and labelling during wet production (laboratory reduction). Due to radiological considerations, the techniques are most suitable for laboratory studies either on particle mobility or reactivity, especially where high concentrations of NPs would be necessary in order to measure low concentrations of particles or Fe in the liquid phase, or those where the location of NPs is required. However, theoretically, the techniques should also be applicable for studies of behaviour in field conditions. At present the techniques

are being explored for applications in laboratory studies of nanoparticle-biofilm interactions (neutron activation) and Carbolron mobility (Tc-99).

3.4.1 Neutron Activation

Neutron activation can be applied to radiolabel any dry NP and has been applied to available NanoRem materials (Nanofer Star, Carbolron, biomagnetite, zeolites). Labelling with iron isotopes during wet production (laboratory reduction) has also been demonstrated. Particles show high variability in specific activity following neutron activation, largely due to differences in the presence of other elements with varying neutron-cross section. In addition to the primary label of Fe activation products (Fe-59 and the shorter half-life Fe-55), other trace elements provide activation products with sufficient efficiency to enable use in tracing (Table 3.5). The presence of these additional activation products can be exploited in particle tracing since it helps to distinguish pristine from dissolved particles. Based on attained specific activities of 2MBq/mg, absolute detection limits of a few fg Fe are achievable.

Table 3.5: Activation products and half-lives (Nanofer STAR)

Element	Label/Activation Product	Half-life
Fe	Fe-59	44.5 d
Eu	Eu-152	4947 d
Co	Co-60	1925 d
Mn	Mn-54	312 d
Ce	Ce-141 (Ce-144)	32.5 d (285 d)
Cr	Cr-51	27.7 d
Zn	Zn-65	3.26 d

3.4.2 Tc-99m

A range of Fe-based nanoparticles being used in the NanoRem programme can be labelled easily with the gamma-emitting metastable isotope of technetium, Tc99m (half-life 6 hours), commonly used for medical imaging. Nanoparticles of carbo-iron, nZVI and biomagnetite were shown to remove technetium (VII) and reduce it to Tc (IV), effectively labelling the nanoparticles as shown figure 5. These particles can now be imaged directly using the same gamma camera, but in dynamic flow-through column studies. These experiments will be conducted following the successful completion of targeted WP3 and 4 experiments in Manchester, and with the collaborating team in Leipzig.

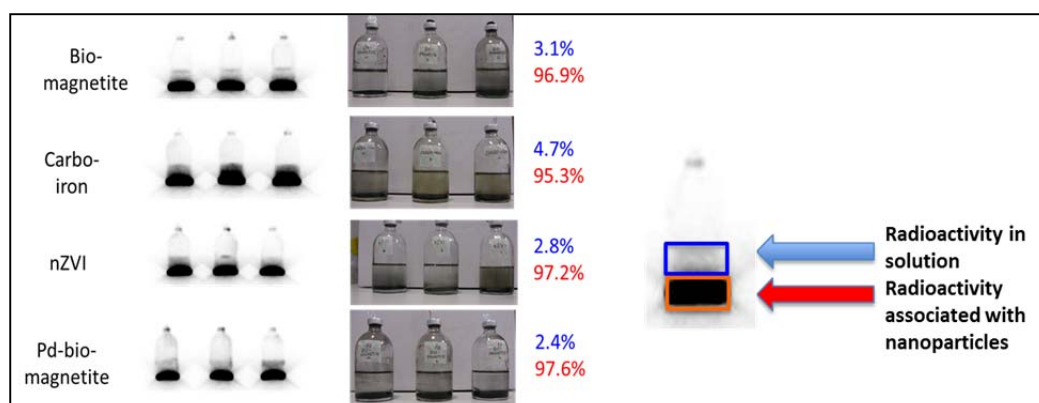


Figure 5: Radiolabelling with Tc-99m.

3.5 Micro Tomography (MicroXCT)

3D Xray micro-computed tomography (MicroXCT) is a direct measurement technique that enables a three-dimensional (3D), non-destructive, spatially-resolved investigation (about 1 μm) with no specific specimen preparation requirement (e.g. drying), and without interpolation or hypothesis on pore geometry. Analysis of columns of sediment using 3D micro XCT (MicroXCT-400, Xradia, USA) from the Equipex NanoID platform has been optimized for Fe-based NPs, and the data treatment using the AVISO® software has been improved. The technique is well suited for localization of nZVI nanoparticles in columns filled with sand without any sample preparation. The core of sediment can be directly analyzed without any cutting or embedment in resin. Iron is easily discriminated from the sand and its distribution can be observed within the pores of the column (Figure 6). Image treatment using the AVISO® software allows the estimation of the percentage of each phase (sand, pores, iron).

Unfortunately, since it is difficult to discriminate the naturally occurring iron phases in soils and sediments from the iron coming from the nanoparticles, this technique is difficult to apply in the field.

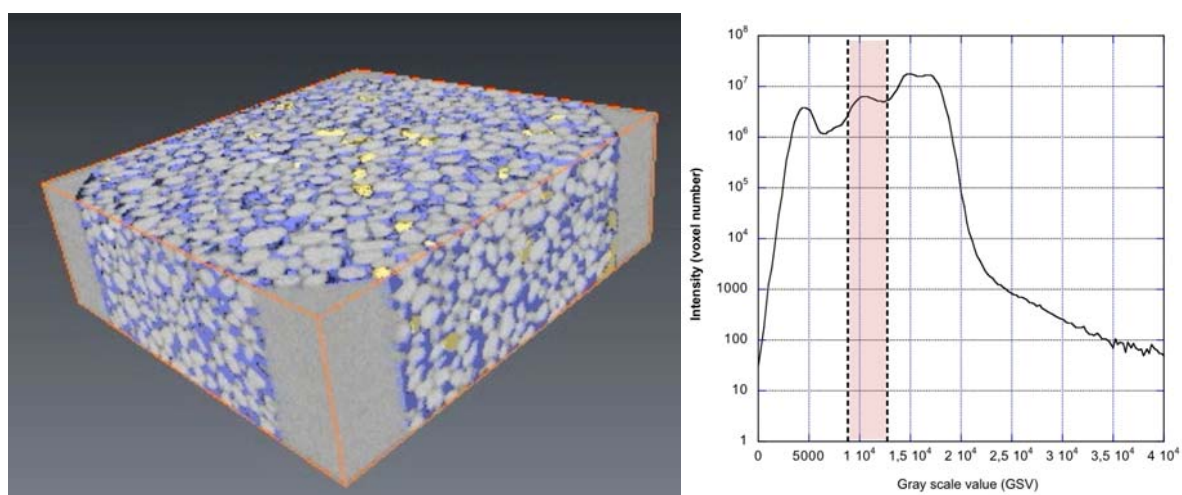


Figure 6: MicroXCT of optimized NF particles in a column of sand during mobility experiment and its grey scale histogram. The sand is in grey, the pores are in blue, and the iron is in yellow. FOV: Field of view. The red area on the histogram represents the iron thresholding.

4 *In situ* measurement

4.1 Magnetic susceptibility

There are very few methods that can detect particles in-situ. One possibility is to use the magnetic properties of iron by detection of changes of the magnetic susceptibility. The University of Stuttgart developed a special probe that can be installed in the subsurface and detects changes in the magnetic properties in the vicinity of the probe continuously. The probe consists of two intertwined inductors, where through the outer one (primary inductor) an alternating electromagnetic field is produced inducing a voltage in the inner inductor (secondary inductor), which is proportional to the magnetic susceptibility of the environment around the probe (see Figure 7).

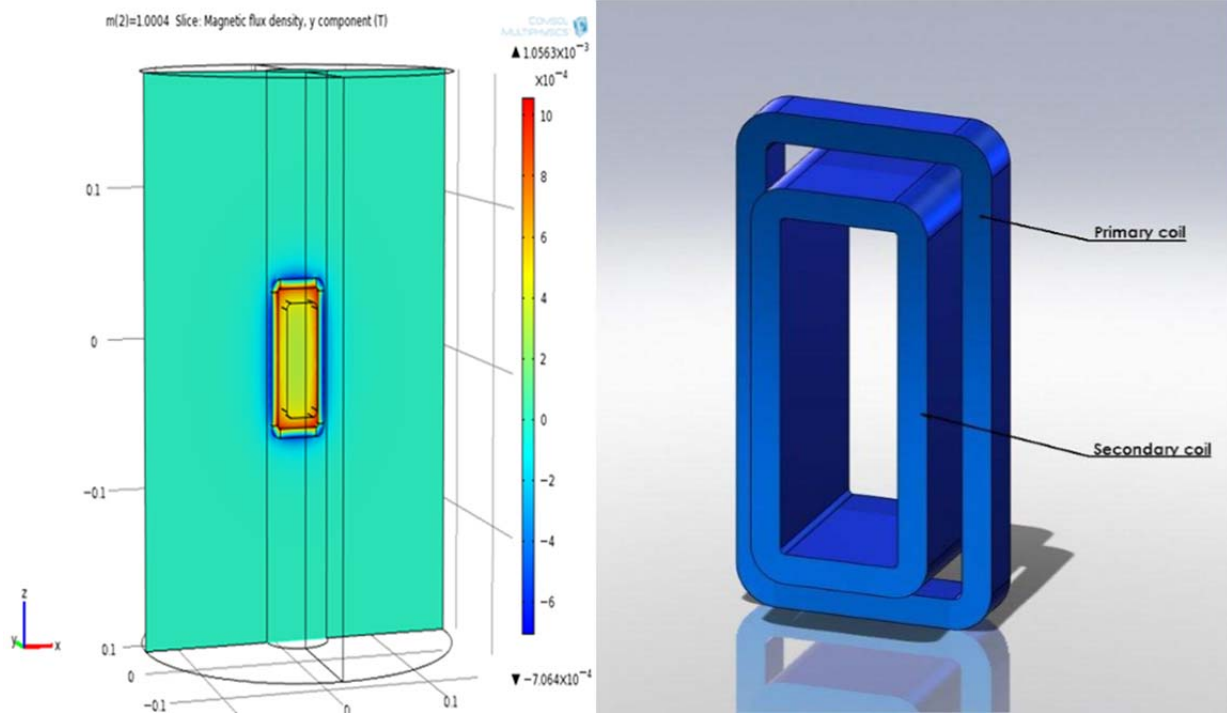
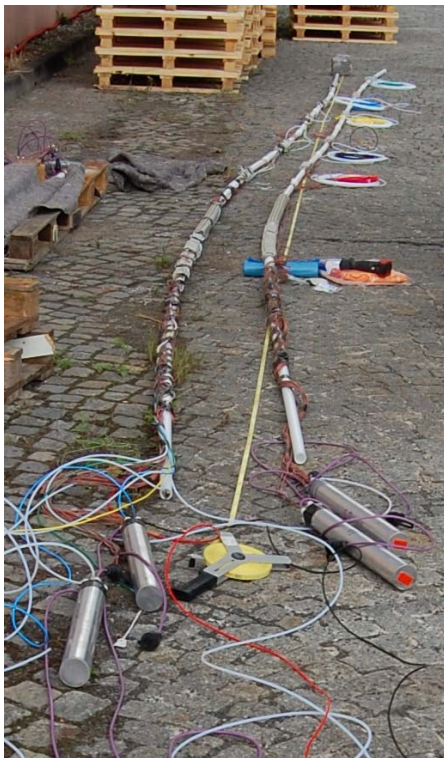


Figure 7: Susceptibility probe, electromagnetic field (left), position and shape of the inductors (right).



The method is limited to measurement of nZVI particles, and at concentrations of 50mg/L. Although recent development indicates it can be applied for Carbolron, albeit with higher levels of detection. The probes can be installed in the subsurface together with a temperature sensor and a special sampling port. Several susceptibility sensors can be lined up in arrays allowing the detection of iron particles and sampling of ground water. Figure 8 shows two arrays before the installation in the subsurface. Such arrays have been installed at the Czech Republic and Hungarian field sites, and pilot studies carried out during injection of nZVI in November 2014. The results are still undergoing analysis.

Figure 8: Sensor-arrays before installation in the aquifer.

4.2 Temperature and redox

In situ measurement of the temperature during the injection is a simple and efficient way of distinguishing between the liquid phase of the suspension and the particles. For long term monitoring of the influence of the particles on the hydrochemical milieu of the aquifer the installation of *in situ*

redox-sensors would be a good choice. Although redox alone would not necessarily indicate the presence of particles, since solution conditions can be reducing without particles (Shi et al., 2011), when combined with pH, temperature, conductivity, etc, and with suitable calibration and background measurements, the sensors could provide important *in situ* information on changes in groundwater conditions. The availability of redox sensors suitable for installation in the subsurface is limited, however a supplier has been located and tests are currently ongoing. Other *in-situ* sensors for detecting milieu parameters such as pH or the oxygen content in the ground water are not stable enough.

4.3 H₂ production

Hydrogen gas measurement can be applied for nZVI tracking by H₂ gas measurement directly in wells, as well as for characterization of either nZVI slurry or nZVI-containing sediment collected from wells using an “acid digestion” method (see section 5.3). The direct measurement method exploits the basic property of iron to reduce water accompanied by the release of H₂ gas. Measurement of the H₂ concentration increase in monitoring or applications wells (namely just above the groundwater level) can be used to trace nZVI. Portable GS1 gas sniffer (Wöhler GmbH, Germany) instruments are available for on-site measurement, or even more sophisticated portable gas detectors. The method works well in application wells, where concentrations of nZVI (typically 1 – 2 g/L) are high enough to permit measurable concentrations of H₂ (i.e., above 10 ppm) over background H₂ content (being up to 5 ppm in most cases). A limitation of this method is that it cannot trace the oxide/oxohydroxides reaction products resulting from nZVI as these common reaction products do not produce hydrogen gas when in contact with water. Moreover, H₂ presence in wells can be also influenced by changes in microbial activity, which can in turn change upon introduction of nZVI, and thus cannot be easily subtracted from background measurement. Nevertheless, provided levels of nZVI are high enough, it can give useful information on the presence of, and changes in levels of reactive Fe.

Table 4.1 shows some representative results of measurements conducted in 3 monitoring wells at Spolchemie, Ústí nad Labem, Czech Republic, before the application of nZVI. In the near future, further measurements will be held in order to investigate and compare the level of hydrogen before and after application of nZVI particles.

Table 4.1: Hydrogen gas measurement- ‘A’ refers to the surface of the wellhead and for ‘B’ the exact point of the measurement was inside the well, above the water level.

Well number		CH ₄	CO ₂	O ₂	lel	H ₂ S	H ₂
		%	%	%	%	Ppm	ppm
PV-129	A	0	0,1	20,7	0	0	0-5
	B	0	1,9	18,7	0	0	0-6
PV-130	A	0	0,1	20,1	0	0	0-6
	B	0	2,2	17,2	0	0	0-6
PV-112	A	0	0	20,4	0	0	0-6
	B	0	0,7	19,4	0	0	0-6

5 On site sampling and measurement

5.1 Size fractionation/ultrafiltration

A variety of filtration techniques can be applied to follow the change in the size distribution of Fe-based particles during injection. On site fractionation avoids the problem of changes in Fe and particle physico-chemical speciation that occur between sampling and measurement, and particularly those due to redox changes (i.e., precipitation, sedimentation, dissolution). The high particle density of injection solutions means that only small samples can be processed with standard filtration techniques before clogging. Hollow fibre filtration methods permit high volumes of samples to be processed down to kDa molecular cut off, and over particle densities over orders of magnitude – upto a few g/l – and allowing processing of up to 1 L samples.

The techniques have been tested at both the tank and the field site injections. Both stock solutions and samples from monitoring wells were fractionated with respect to size (molecular mass using at site filtration (Pall high capacity GWV 0.45µm sampling capsule) and ultrafiltration (Pall microza hollow fiber operating with nominal molecular mass cutoff 10 kDa). Samples were ultrafiltered within 30 mins to 3 hrs after sampling, giving an overview of Fe associated with three different molecular mass fractions: low molecular mass fraction (LMM < 10 kDa); colloids (>10 kDa and < 0.45µm) and particles (>0.45µm). Initial qualitative measurements of the fractions at site can be carried out using spectrophotometric measurements (see 3.2); while quantitative measurements can be performed by ICP-OES. The concentration of colloidal Fe forms such as colloids is derived by difference: colloidal Fe = Fe 0.45µm – LMM Fe.

Table 5.1 shows the Fe concentrations in FeOx stock solutions used at the tank and field experiments, demonstrating the efficiency of the ultrafiltration techniques. The Fe concentration in unfiltered (total), filtered (0.45µm) and in ultrafiltered samples (LMM Fe) from the tank experiment is shown in Figure 9. This demonstrates the marked change in Fe size distribution following injection: the preinjection distribution was dominated by soluble LMM species, while a rapid change in both particulate and colloidal fraction, and a reduction in dissolved fractions due to redox changes, was observable 1 hour after injection.

Samples from both the tank and the field site are currently undergoing analysis of rare-earth elements and stable Fe-isotopes in order to test applicability of these methods for tracking nZVI and FeOx remediation particles.

Table 5.1: Size distribution of Fe in FeOx stock solutions: hollow-fibre ultrafiltration.

	Fe mg/l (unfiltered)	Fe mg/l (ultrafiltered)
Stock FeOx (Vegas)	4400	<0.08
Stock FeOx (Czech)	3500	7

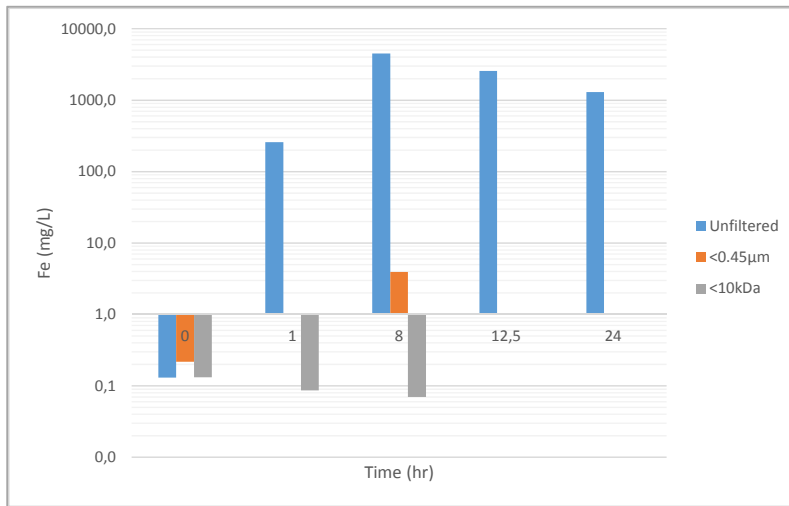


Figure 9: Variation in size distribution of Fe at position 3eD (ca 1 m from injection) in the Vegas tank with increasing time after injection of FeOx NP. Fe concentrations determined by ICP-OES (Perkin Elmer Optima 5300 DV). Analysis of the 0,45 µm and 10 kDa fractions hr is ongoing.

5.2 Turbidity

Turbidity measurements can be applied at site and over a relatively large particle concentration range. To date the method has been tested on nanoscale Fe-oxides (HMGU), and measurements carried out with a Turbidimeter (2100N IS, ISO Method 7027). Calibration has also been carried out for Carbo-Iron (see section 6.3). The required sample volume (undiluted) is 2 to 20 ml, depending on the measurement cell, and the time of measurement about 1 to 2 minutes per sample. Calibration has been carried out with a five-point calibration from 0 (Milli-Q water) to 1000 NTU. All values above 1000 NTU have to be diluted and measured again. Tests in lab scale (batch, column) and in pre-field scale (large scale container experiment Vegas) have been conducted and showed comparable results. The method can be applied over a concentration range of 0.5 mg L⁻¹ to 1.0 g L⁻¹ (depending on the water quality). Based on turbidity measurements the distribution of the Fe-oxide particles was monitored during and after the injection (20 hours after injection: Figure 10).

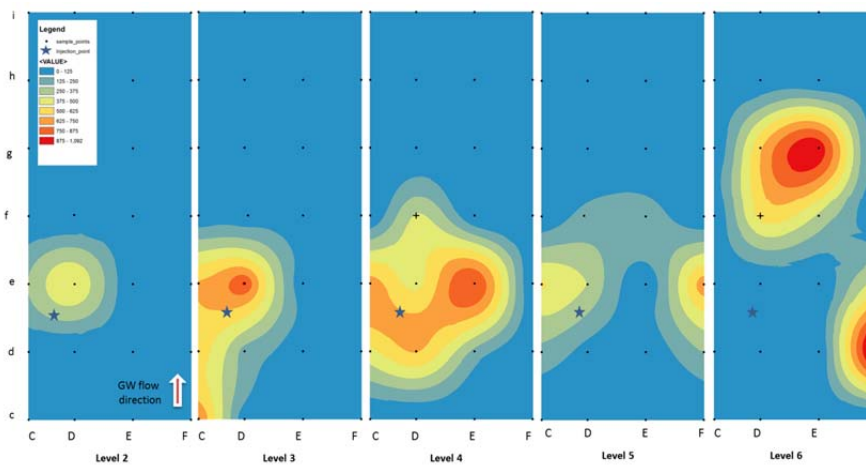


Figure 10: Turbidity data indicating particle distribution at different depths (Level 2-6) 20 hours after injection of FeOx at the VEGAS Tank Experiment.

5.3 Fe content and conductivity

Providing the chemical properties of injection suspensions are significantly different from that in ground water, a number of standard chemical techniques can be applied to follow the fate of suspensions during injections. As described in sections 3 and 4, these can include temperature, redox, conductivity as well as total Fe content. As for turbidity, many methods can give results within a few minutes of sampling. For example, during the tank experiment, the injected suspension had an elevated electrical conductivity (>1 mS/cm), while the LSC groundwater only had an EC of ~ 320 $\mu\text{S}/\text{cm}$, enabling a good overview of the movement of the liquid fraction (Figure 11). Analysis of total Fe content gave one of the more reliable pictures of particle distribution, and was used by all analytical groups as a control of the other sampling methods.

While acid digestion followed by ICP-OES gives a quantitative measurement of Fe content, a rapid on site assessment can be provided with spectrophotometric measurements. With the aid of a portable spectrophotometer (e.g., DR 2000) measurement of Fe content in 25 ml samples can be provided within 15 mins. Information on both total Fe and Fe^{2+} , based on complexation with FerroZine® and 1.10 phenanthroline, respectively, can be provided at concentration ranges of 0.2-200 mgL^{-1} (or greater with dilution) The measurement of total Fe will be underestimated if the Fe is associated with large particles, although it is possible to exploit the relatively slow reaction time of particle bound Fe, and the rate of change in signal intensity, to obtain additional information on particle size and concentration. Studies are ongoing to give a more quantitative assessment. In the VEGAS tank experiments, the low total Fe and dissolved Fe concentrations (<0,5 mg/L) made tracking using total Fe relatively straightforward, in both total and size fractionated samples. The Fe concentrations at the Spolchemie field site were more variable, but still spectrophotometric analysis gave sufficient sensitivity to pick up particle distribution in monitoring sites.

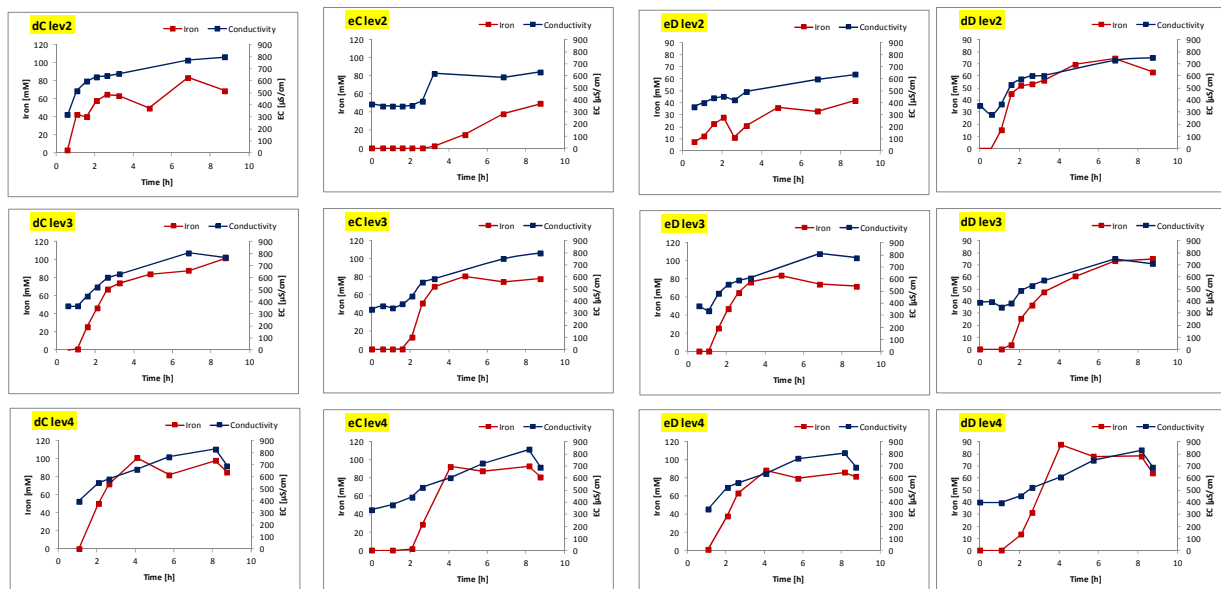


Figure 11: Iron total and electrical conductivity measured in the four monitoring wells around the injection well over 3 depth layers (level2 – level4) and over the timeframe of the FeOx nanoparticle injection at the VEGAS tank experiment.

5.4 Mossbauer: nZVI

Transmission ^{57}Fe Mössbauer spectroscopy is an important tool for a characterization of nZVI (both in dry powders and aqueous slurries) and it represents an unique technique for probing the $\text{Fe}^0/\text{Fe}_{\text{tot}}$ ratio yielding precise values of the relative Fe^0 content. While the Mössbauer spectrometer is compact, and portable the main disadvantage lies in the relatively long counting times (typically about 1 day per sample of nZVI) during which the measured sample could further oxidize. This drawback is compensated by measuring samples under protective atmosphere, as the whole spectrometer could be installed e.g., in a glove box (Filip et al., 2014). Alternatively, pre-concentrated nZVI-containing samples could be fast frozen and measured at low temperatures (optimally at L_{N_2} temperature) utilizing a special cryogenic system which slows oxidation of nZVI (Filip et al. 2007). The low-temperature measurements are further beneficial in the case when reaction products of nZVI are amorphous (therefore hard to detect by XRD). The other very important benefit of this method is its iron-selectivity (Sharma et al. 2014). Therefore, ^{57}Fe Mössbauer spectroscopy could be applied for complicated samples like the direct observation of nZVI oxidation in soil samples collected from either laboratory column experiments or field tests.

Transmission ^{57}Fe Mössbauer spectra can be collected at a constant acceleration mode with a $^{57}\text{Co}(\text{Rh})$ source (1.85 GBq). Magnetically pre-concentrated slurries are fast frozen in a liquid-nitrogen bath and measurements carried out at 250 K and in external magnetic field of 0T for 1 day per sample. Alternatively, fast-dried (e.g., lyophilized) powder samples can be prepared under protective N_2 into the form of conventional absorber ($\sim 5 \text{ mg Fe cm}^{-2}$) and measured at RT using a spectrometer located directly in the glove-box. In both cases, the isomer shift values are calibrated against an $\alpha\text{-Fe}$ foil at RT. The spectra are fitted with Lorentz functions. The effects of non-ideal absorber thickness and variable recoil-free fractions for iron atoms in non-equivalent structural sites of different phases are expected to be within experimental errors (hyperfine parameters $\pm 0.02 \text{ mm s}^{-1}$, relative spectral area $\pm 3 \%$).

Figure 12 shows a typical spectrum and Table 5.2 shows the values of the Mössbauer hyperfine parameters, of a sample collected from Spolchemie, Ústí nad Labem, Czech Republic one month after application of nZVI. Results show that the iron detected, exists in the oxide phase as based on the typical characteristics of iron oxide (defined from doublet component).

Table 5.2: Values of the Mössbauer hyperfine parameters, derived from the least-square fitting of the room-temperature Mössbauer spectrum of the sample PV-130_10.12.2014, where B_{ext} is the induction of the external magnetic field, δ is the isomer shift, ΔE_{Q} is the quadrupole splitting, B_{hf} is the hyperfine magnetic field, and RA is the relative spectral area of individual spectral components identified during fitting.

Sample	Component	δ ± 0.01 (mm/s)	ΔE_{Q} ± 0.01 (mm/s)	B_{hf} ± 0.3 (T)	RA ± 1 (%)	Assignment
PV-130_10.12.2014	Doublet	0.42	0.61	-----	100	Fe^{3+}

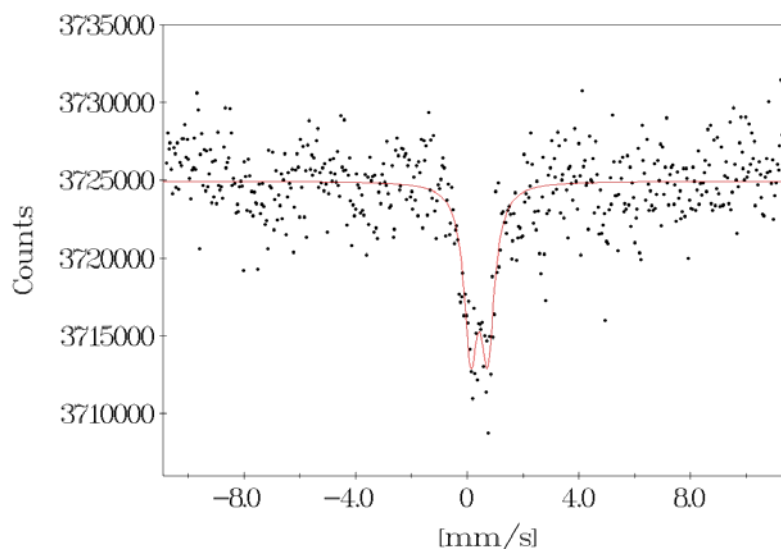


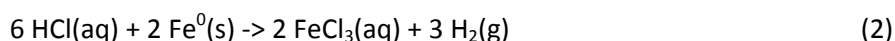
Figure 12: Room-temperature Mössbauer spectrum of a sample collected from Spolchemie, PV-130, 10.12.2014.

5.5 H₂ Production: Acid Digestions

The acid digestion method for measurement of Fe⁰ content in nZVI-containing slurry utilizes the well-known process of metal acid digestion accompanied by hydrogen gas evolution. The process of *acid digestion* of micron-sized iron particles is typically very slow and requires up to 20 days until the reaction is completed. Nevertheless, when working with the particles in the diameter range well below 500 nm (i.e. as typical for all commercially available nZVI materials; Fu et al., 2014), this process is significantly faster and all iron particles are usually dissolved within few minutes. The method is specific to nZVI as iron-oxides produce no hydrogen under these conditions. The reaction of the nZVI with either potassium bisulfate (KHSO₄) or hydrochloric acid (HCl) proceeds according to the following reactions:



or



The weight and the concentration of nZVI in the slurry (either Fe⁰/Fe_{tot} ratio, or percentage of Fe⁰ in slurry, i.e., w/w content of "active" metallic iron) can be consequently calculated from the volume of the evolved hydrogen. Based on equation (1), 55.85 g of zero-valent iron can evolve 22.41 dm³ of hydrogen at 273K (24.5dm³ at ambient temperature).

The apparatus used consists of a standard reaction glass bottle capped with a septum (for injection of nZVI slurry) and filled with saturated acid, connected to either a graduated U-tube or a graduated cylinder placed vertically and further connected to storage vessel. After the completed reaction (typically few minutes in the case of nZVI particles well below 500 nm) the hydrogen volume is read directly. The Fe⁰/Fe_{tot} ratio is determined from the exact mass of the dispersed phase (i.e. nZVI particles) in the studied slurry. This can be derived from the nZVI weight prior to mixing with deionized water, or the air-dried solid sample can be annealed at 900 °C for 1 hour in air in order to oxidize all iron into hematite (α-Fe₂O₃) and then weighted.

The advantages of the test are its inexpensiveness and simplicity - the apparatus can be constructed and easily operated at any chemical laboratory or at remediation sites. The method gives information on both the Fe₀/Fe_{tot} ratio (similarly as Mössbauer spectroscopy and XRD), but also actual content of Fe₀ in aqueous slurries.

5.6 X-ray powder diffraction: nZVI

X-ray powder diffraction is an accepted and widespread tool for characterization of the phase composition (i.e. the crystal structure and quantitative phase analysis) of crystalline solids, including nZVI (Clearfield et al., 2008). It also provides information on particle size according to the broadening of diffraction peaks or when combined with small-angle X-ray scattering (SAXS) (Williams et al., 2005). Sample preparation procedures for measurement, data collection and processing have been reviewed in detail many times (Buhrke et al., 1998). Specific challenges linked to nZVI sample preparation and measurement arise from the fast oxidation of nZVI in air (Filip et al., 2014). In order to test method reproducibility, two protocols were followed for either wet nZVI samples (i.e., magnetically pre-concentrated slurries) or dry nZVI powders (see below). Moreover, successive short scans using of fast solid-state detector provide a unique insight into the possible process of nZVI oxidation during sample measurement (typically acquired within less than 1 hour) accompanied by spontaneous drying of the slurry. For the subsequent quantitative phase analysis utilizing full-profile fitting (i.e., rietveld refinement) one can use either the first fast scan collected at the beginning of nZVI drying/oxidation or sum up all collected scans when no phase changes took place in the course of successive measurements.

X-ray diffraction (XRD) patterns were recorded on a X'Pert PRO (PANalytical, The Netherlands) instrument in Bragg-Brentano geometry with iron-filtered CoK_α radiation ($\lambda = 0.178901$ nm; 40 kV and 30 mA) equipped with a fast X'Celerator detector and programmable divergence and diffracted beam anti-scatter slits. Figure 13 shows the pattern recorded with the above experimental setup, on a sample collected from the Spolchemie field site, about one month after nZVI injection. The main crystalline phases identified include: SiO₂, Goethite (FeOOH), Anatase (TiO₂) and Anorthite (Al_{1.8}Ca_{0.8}Na_{0.2}O₈Si_{2.2}).

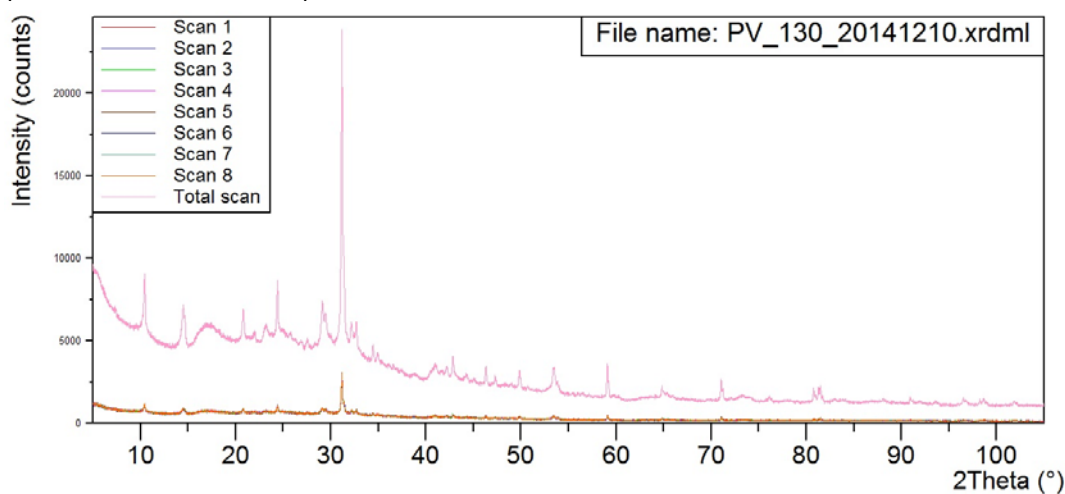


Figure 13: XRD pattern of the sample PV_130_20141012 collected from Spolchemie, PV-130, 10.12.2014.

5.7 ICP-MS and rare earth elements

Inductively coupled plasma mass spectrometry (ICP-MS) is capable of detecting low concentrations of metals (trace and even rare earth elements) and several non-metals on small sample volumes (in the scale of few mL). Its application in tracking nanoparticles requires an analysis of the remediation particles and comparison with background measurements on water/sediment samples from the injection site. This can allow a set of elements to be selected, whose ratios are typical for nanoparticles but not present (or present at very different ratios) in groundwater/sediment at the site. Alternatively, it could be possible to dope the nanomaterials with selected rare earth elements, or pairs of elements.

Preliminary tests of the method have been run for FeOx and nZVI particles, both in the tank experiment and the Spolchemie site. To date measurements have been carried out on stock solutions and background samples in order to identify potential tracing elements (Figure 14). Full details of preliminary results of rare-earth elements in a selection of samples is given in Appendix 1. For nZVI it appears that the ratios of REE/Fe are 5-6 orders of magnitude lower in nZVI than in site groundwater for a number of RRE. Thus changes in these ratios could be indicative of the presence of nZVI. In the next step, the same measurements will be performed on broader set of samples collected before and after application of nZVI particles into the groundwater in order to monitor the transport of nZVI in groundwater.

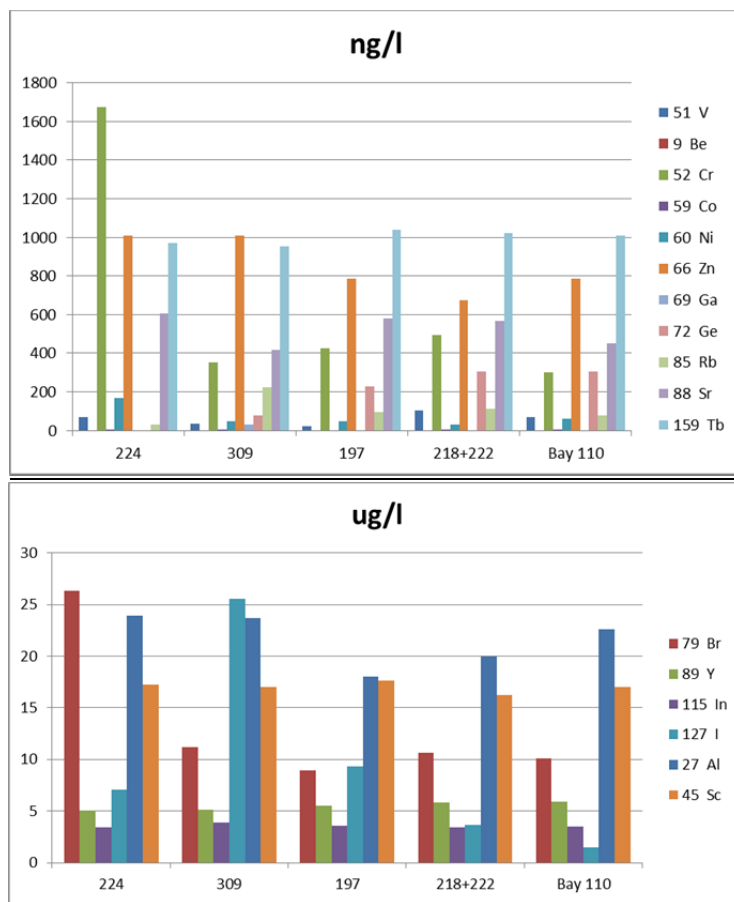


Figure 14: ICP-MS determination of the concentration in ng/L of selected elements in 5 different batches of nZVI iron nanoparticles.

6 Carbolron and Fe zeolites

6.1 Carbolron: Fe/C ratios

Carbo-Iron can be traced using the carbon and iron contents of water and sediment samples. Particulate organic carbon (POC) has been used as a measure of the particle concentration at the lab scale to detect Carbo-Iron particles in effluent streams and as deposited agglomerates in sediment matrices. The POC can be easily derived from carbon-containing particle suspensions after removing the inorganic and purgeable organic carbon and subsequent filtration over $< 0.2 \mu\text{m}$ membrane filter. The detection limit for particle concentration is 5 mg/L, making it suitable for lab studies, and applicable at field sites providing that the POC can be distinguished significantly from naturally present carbonaceous compounds present. Additionally, the total iron content is a suitable parameter for tracing Carbo-Iron colloids, with a nominal loading of 30 wt-% of total iron (see section 3.2).

Since both (carbon and iron) are ubiquitous elements, concentrations alone might not be enough to characterize a complex sample obtained from a field site. Therefore, the ratio of iron concentration to concentration of particulate carbon ($c_{\text{Fe, total}}/c_{\text{POC}}$) can be a valuable parameter for particle detection regardless of the natural background of both elements. Oxidation of metallic iron to oxidic species will change the elemental composition, but, providing there is no significant leaching of iron, the ratio will not change significantly. In a first pre-test for field application, underground Carbo-Iron particle screening has been carried out. Figure 15 shows an example for a depth profile of the element concentrations for carbon and iron found at a site where Carbo-Iron had been injected previously. The measuring points where Carbo-Iron has been applied earlier clearly showed a different $c_{\text{Fe, total}}/c_{\text{POC}}$ pattern (blue area in Fig. 15) than those which never came in contact with the particles (red dots).

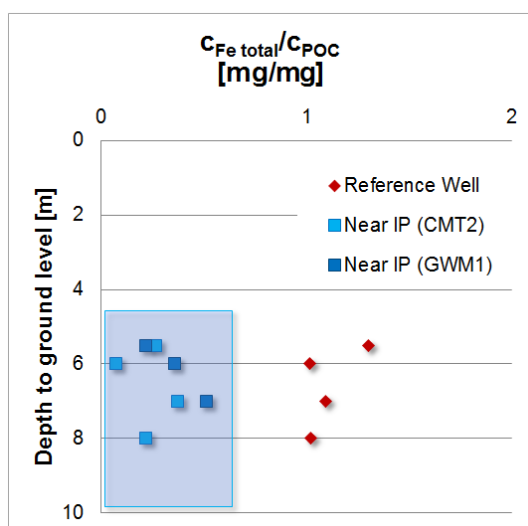


Figure 15: The ratio $c_{\text{Fe, total}}/c_{\text{POC}}$ at CMT measuring points (with depth profile) at a site in Celle/Bergen.

(IP = injection point, CMT2 and GWM are measuring points)

6.2 Carbolron: Temperature Programmed Oxidation (TPO)

Temperature-programmed oxidation (TPO) of solid sediment samples utilizes the fact that the immediate vicinity of the carbon has an effect on the carbon-specific oxidation temperature. In case of Carbo-Iron, the embedment of iron decreases the incineration temperature significantly in comparison to pure

powdered activated carbon (Bleyl et al. 2012). One can take advantage of this temperature shift to detect carbon-based particles within a complex matrix containing a natural carbon background. Figure 16 shows the specific incineration patterns in air atmosphere for Carbo-Iron particles (H2-CIC ; HT- CIC and aged HT-CIC), the raw material activated carbon (AC), the colloid stabilizer CMC and a coal-derived humic acid as a model compound for natural carbon background.

CMC shows two narrow decomposition peaks at 294°C and 619°C clearly separated from the Carbo-Iron incineration peak, which occurs at 453°C for H2-CIC and in the range of 550°C to 560°C for the pure respectively the aged high-temperature products (HT-CIC). With a view to the large-scale production, the high-temperature synthesis pathway is preferred; thus the development of the analytical method for particle tracing has been focused on HT-CIC. The humic-acid oxidation leads to broad peaks at 317°C and at 455°C superimposed by the incineration peak of H2-CIC but will not interfere with the combustion peak of aged HT-CIC. Additionally to potential colloid stabilizers, natural carbon sources as carbon black or fulvic acids will be subject of further investigations. Experiments with the original sediment of a site have to be conducted in order to avoid interference of its soil organic matter fraction with Carbo-Iron detection by this method. Another approach can be the acidic pre-treatment of the solid samples in order to remove the iron content. This should split up the close connection between the carbon backbone and iron which is responsible for the iron-catalysed carbon incineration. Iron removal should shift the oxidation peak for Carbo-Iron to higher temperatures, possibly to the range of activated carbon combustion. Carbonates will also be removed by means of acid pre-treatment. The CMC combustion peak close to the peak for activated carbon should be unproblematic, since the mass of CMC adsorbed to Carbo-Iron is very low (maximum loading < 10 wt%).

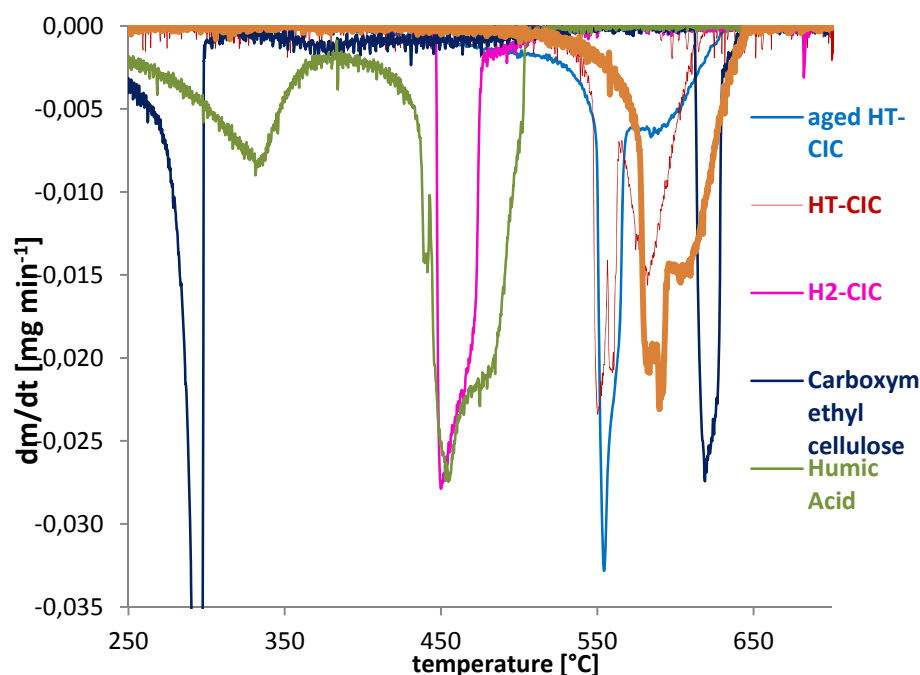


Figure 16: Temperature-programmed oxidation (TPO) of carbonaceous materials in a thermogravimetric balance (TGA-50 Shimadzu: air flow rate 50 mL/min; $m_{\text{sample}} = 6 \dots 16$ mg; $\Delta T: 10$ K/min; $T_{\text{max}} = 700^\circ\text{C}$).

The main challenges that remain are sample preparation of natural heterogeneous aquifer sediment to achieve representative results for the sediment loading with carbon species and the detection of low-concentrated particle fractions ($\ll 0.1$ wt-%) in complex matrices. In order to demonstrate proof of concept for TPO, real sediment samples from the large scale flume experiment and the field-test site (Balasagyarmat, Hungary) will be subject to further investigations in the following project period.

To quantify Carbo-Iron particles immobilised on sediment grains, predefined loadings of aged HT-CIC on the NanoRem standard material M.I (Dorsilit®) in a typical expected range of 0.1 wt% up to several wt% has been studied. A linear calibration curve for the relative mass lost (normalized to m_{sample}) as a function of the mass loading of Carbo-Iron was obtained.

The obtained results show the principle applicability of the TPO approach for qualitative and quantitative particle tracing in lab tests with model sand and aged Carbo-Iron. The detection limit for the particle loading was calculated on the basis of the specific incineration peak with 0.3 wt%. The combination of TPO with gas analysis (formation of CO_2 and CO) is an additional promising tool to unequivocally trace particles in natural matrices and increase the sensitivity, reliability and applicability for real sediment samples from field sites. As an off-site method the TPO approach can be understood as complementary tool, which contributes to existing on-site methods.

6.3 Fe-Zeolites

The application of colloidal Fe-zeolites for in-situ remediation is still in the lab-scale research stage, however a number of detection methods have been initiated. Since Fe-zeolites basically consist of the elements silicon, aluminium and iron, which are ubiquitous in the environment, element detection techniques can only be applied at relatively high particle concentrations. As for other Fe-based particles, the main standard methods are turbidity (measuring absorbance at 860 nm) and total iron measurement after acid digestion. Figure 17 shows the calibration curves for absorbance measurements over the concentration range of 0.1 to 5 g/L Fe-BEA-35. With respect to total Fe measurements, to completely dissolve the zeolite-bound iron from Fe-BEA-35, a suspension with 4 M HCl has to be shaken overnight (≥ 18 h). Dynamic light scattering (DLS), nanotracking analysis (NTA) and laser diffraction were tested for analysis of particle size distribution of zeolite suspensions. Applicability of NTA and DLS is hampered by the fact that most of the available zeolites are polydisperse and contain a size fraction $> 1 \mu\text{m}$. Laser diffraction analysis was identified as suitable method for particle size analysis of zeolite suspensions.

Other characteristic features of the native Fe-zeolites which could be utilized for *indirect* quantitative determination of their content *in sediments* are: i) high specific surface area, ii) activity for H_2O_2 decomposition and iii) high adsorption affinity towards small organic molecules. Approach i) relies on determination of BET area by N_2 adsorption experiments. For acid washed Ottawa quartz sand (0.59 – 0.84 mm, Figure 18) a limit of detection for this method of 0.03 wt% Fe-BEA-35 was determined, with this mass fraction of Fe-BEA-35 causing a twofold increase in BET area compared to the original sand ($0.08 \pm 0.02 \text{ m}^2/\text{g}$, BET surface area of Fe-BEA35: $612 \text{ m}^2/\text{g}$). For sediments with a larger fraction of fines the DL is expected to be higher. A disadvantage of the method is the low sample throughput (2 samples/day).

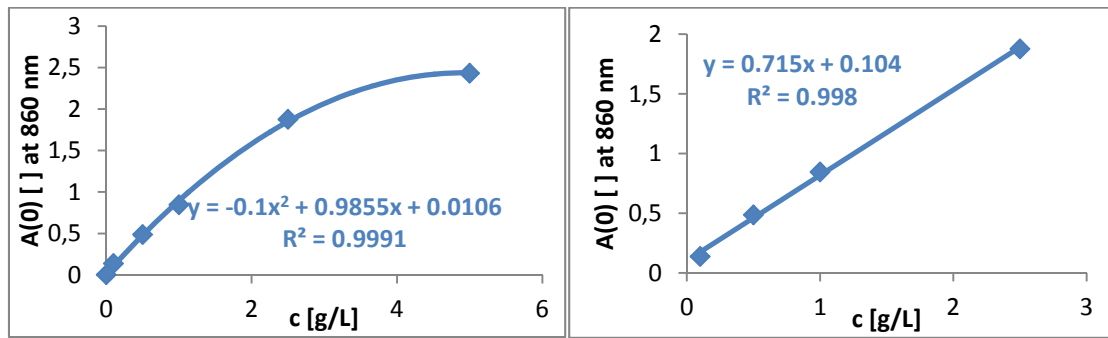


Figure 17: Calibration curves for determination of the concentration of Fe-BEA-35 in aqueous suspension by means of measurement of absorbance at 860 nm (UV-Vis instrument Varian Cary 300) (right figure for concentration range 0.1 – 2.5 g/L).

With respect to H_2O_2 decomposition (approach ii) catalytic activities of the Fe-zeolites were compared with those of the porous media used in NanoRem, i.e. M.I (Dorsilit® 8 – acid washed) and M.II (middle sand) as well as untreated Dorsilit 8. In case of Fe-BEA35 a mass fraction of only 0.01 wt% of Fe-zeolite on M.I causes already a two-fold increase in the rate constant for H_2O_2 decomposition, set as detection limit. However, untreated Dorsilit 8 as well as M.II show relatively high activities for H_2O_2 decomposition, so that high Fe-zeolite concentrations are needed to cause a significant increase. Thus, H_2O_2 decomposition, even though it can be applied for lab experiments with cleaned sand, is not a suitable quantitative parameter for determination of Fe-zeolite concentration in real aquifer sediments.

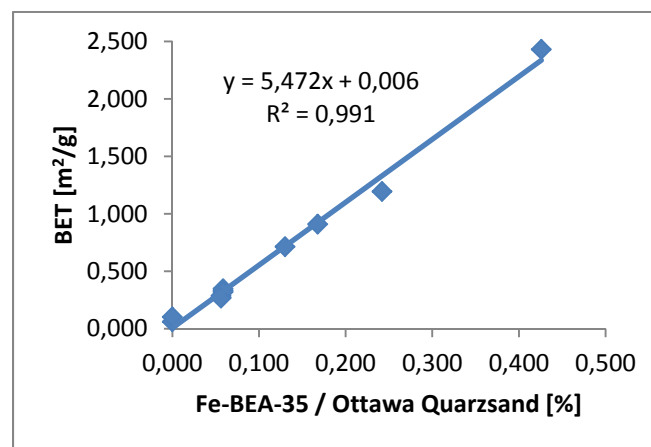


Figure 18: Calibration curve for determination of Fe-BEA-35 on Ottawa quartz sand by BET analysis.

For testing approach III) suspensions of M.I with various amounts of Fe-BEA-35 in 10 mM KNO_3 solution containing 20 mg/L of MTBE were prepared and the concentration of MTBE in the aqueous phase was analysed after 24 h. A linear correlation between c_{total}/c_e (ratio of concentration of total MTBE added and equilibrium aqueous phase concentration) and mass fraction of Fe-BEA-35 in relation to porous medium M.I was obtained within the relevant range of 0.1 to 1 wt% (Fig 19), showing a nearly constant sorption coefficient for MTBE on the zeolite ($c_{e,MTBE} = 4 - 20$ mg/L). In general, the DL of this approach depends on the difference in K_d for the original sediment and the zeolite. Results showed a K_d for Fe-BEA-35 of 1500 L/kg, compared to the K_d for sorption of MTBE to the original porous medium M.I (and also untreated Dorsilit 8) of 0.17 L/kg. For Fe-BEA-35 on M.I the DL is 0.05 wt%. In general, the DL of this approach de-

depends on the difference in K_d for the original sediment and the zeolite. The latter can reach values in the order of 10^5 L/kg for hydrophobic zeolites so that the DL in this case can be even lower. Sediment properties such as high content of fines or natural organic matter (NOM) can increase background adsorption by the sediment to some extent and thus slightly increase the detection limit for this approach. Nevertheless, sorption coefficients of MTBE on NOM are expected to be lower by two orders of magnitude than $K_{d,Fe-BEA-35}$ based on the low hydrophobicity of MTBE ($\log K_{ow,MTBE} = 0.94$). In addition, before conducting the adsorption experiment, sediment samples could be calcined in air to remove any organic material and treated with dilute acid to remove inorganic carbonate precipitates which could interfere with the analysis. Target contaminant adsorption appears most suitable among the indirect methods for determination of Fe-zeolite content in sediments with respect to handling and DL. However, it's not a trace method but only applicable close to the targeted range of zeolite concentration on sediment of 0.01 to 1 wt%.

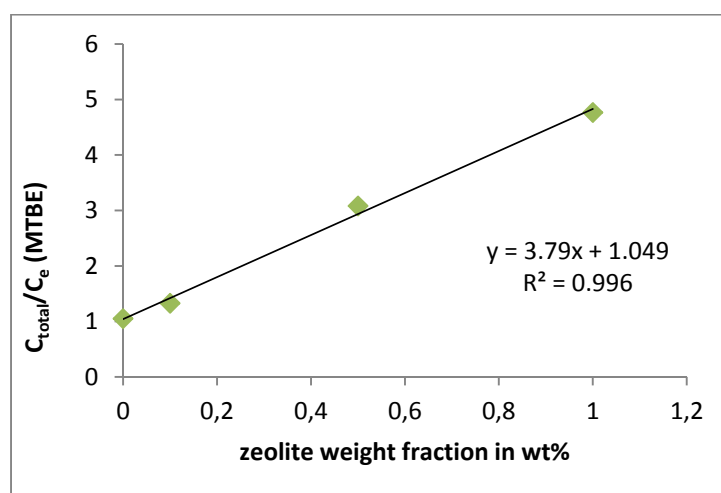


Figure 19: Calibration function for indirect determination of zeolite weight fraction (Fe-BEA-35) in sand (M.I) via adsorption of MTBE (c_{total}/c_e = concentration of total MTBE added / equilibrium aqueous phase concentration)

Finally, with respect to *direct* methods for Fe-zeolite detection a fluorescence labelling approach was studied. A fluorescence-labelled zeolite should overcome the disadvantages of turbidity measurement as means of quantifying zeolite content in suspensions. Furthermore, it can be used to investigate zeolite loaded sediment by confocal fluorescence microscopy and obtain insight into filtration details and transport pathways of injected zeolite particles. A 'ship-in-a-bottle' synthesis approach was used to produce a fluorescent BEA-zeolite, whereby fluorescein is synthesized inside the zeolite framework (Figure 20) from inexpensive educts by a simple solid phase reaction at elevated temperature and reduced pressure. It is intended to add the fluorescent zeolite particles to the functional Fe-loaded zeolite particles in a ratio of 1-2%, acting as a label for detection. Thus, we need to verify that the fluorescent particles are representative for the overall particle ensemble.

So far the synthesis has proved successful for Fe-free zeolite BEA-35 (having otherwise identical properties to Fe-BEA-35). Work is ongoing including a further characterization to ensure that the Fe- and the FLU-loaded BEA-35 zeolites behave identically with respect to transport parameters.

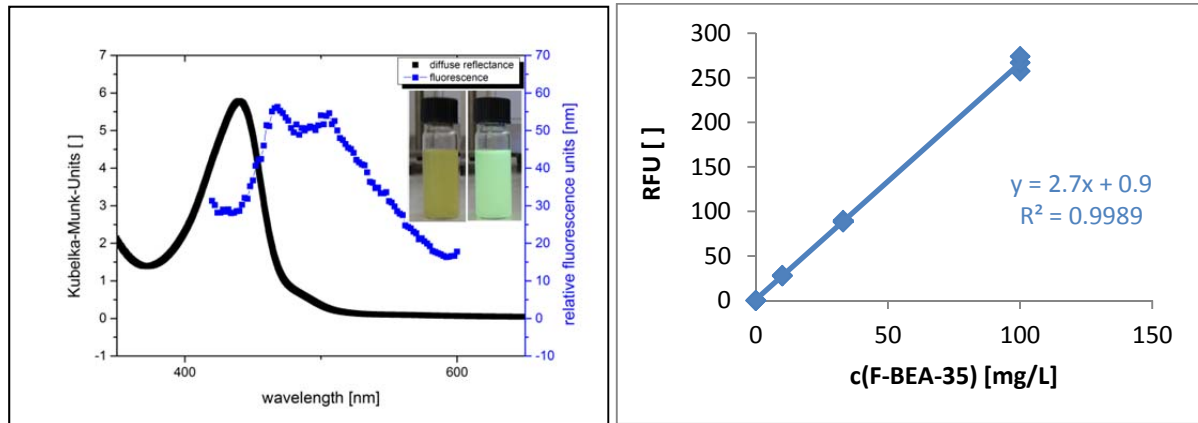


Figure 20: UV-Vis spectrum in diffuse reflectance mode for fluorescent zeolite (FLU-BEA-35); its fluorescence spectrum ($\lambda_{ex} = 385$ nm, suspension in deionized water) and photo of suspensions under daylight (photo left) and UV light (photo right) (left figure); Calibration data for fluorescence detection of FLU-BEA-35 in deionized water (right figure).

7 Summary: Applicability of the Methods

A wide variety of methods are available for monitoring and characterising nanoparticles in laboratory and field experiments. The methods are complementary and applicability depends on both the particle utilised and the question to be asked. Six of the WP6 partners have participated in method development tests during joint fieldwork at large scale tank experiments and field sites are ongoing. Analysis of samples collected at the sites are ongoing, and further insights are expected from follow-up sampling and field tests to be carried out in 2015.

A summary of the various methods, detection limits and limitations is given in Table 7.1.

Monitoring of particle dispersion during injection phase: Results from tanks and field applications show that the detection of particle loads 0.5-5 mg/L during the injection process is relatively straightforward, with a combination of at site sampling, and analysis of suspensions (turbidity, conductivity, redox, temperature and Fe content). This is sufficient to follow the distribution of particles during injection, but follow-up data analysis is required for a quantitative assessment and design of standard operating protocols. Given the relatively low toxicity of Fe-based particles to organisms (See IDL5.1), the current detection limits should at least be sufficient for demonstrate potential ecological impact. On-site measurements of turbidity, conductivity and Fe concentrations using spectrophotometry are all relatively fast and cheap methods. The instrumentation required for on site measurements is portable and not expensive.

Magnetic susceptibility, redox and H₂ measurements have the potential to be applied as *in situ* techniques, but have relatively high detection limits, in the order of 10s of mg/L, and are still under assessment for field performance. While instrumentation costs for the magnetic array sensors are higher than those for the above methods (ca. 1000 EURO for the hardware and 1000 EURO for the electronics), they are one of the few truly *in situ* methods and have the advantage of giving continuous logging data.

Monitoring of renegade particles More sensitive methods are required to distinguish lower concentrations of Fe-based NPs from background matrix, but tests and developments of a variety of methods (SedFFF, ICP-MS rare earth analysis, Fe-stable isotopes) is ongoing. While detection limits of these methods are known to be extremely low in clean media, the performance will be dependent on site specific parameters. Nevertheless, preliminary tests in both the VEGAS tank experiment and Spolchemies show measurability down to a sub-mg levels. Full reports of the performance of these methods will be provided in the next deliverable.

Post injection monitoring. In addition to the methods used during injection, Mossebauer and H₂ production can give useful additional information on the time dependent changes in particle state and reactivity.

Table 7.1: Summary of Applicability of Selected Nanoparticle Characterisation Methods

Method	Concentration range	Size Range	Comments/Limitations
Tested for at site or <i>in situ</i> applicability			
Turbidity (TurbidScan)	0.5 mg – 1 g/L		Tested for FeOx and Fe-zeolites. Applicable in the field but detection limits depend on background turbidity measurements.
Fe-content (ICP-OES, spectrophotometry)	µg – g/L	NR	Applicable for all particles. Applicable in the field (spectrophotometer), but detection limits are dependent on site background concentrations.
Magnetic susceptibility	50 mg/L – g/L		Only nZVI. <i>In situ</i> measurements, but low mobility of nZVI means that detection will be contingent on the sensor being placed in a location where the particles will migrate. Some limitations in placement, eg under rail tracks.
Direct H ₂ Measurement	> 10 mg/L	NR	nZVI only. Cannot trace oxide/hydroxide reaction products. On site applications dependent on background measurements and redox
Ultrafiltration	µg – g/L	ca 10 – 450 nm	All particles. Field sampling technique. Used in combination with other techniques for separating dissolved and particulate Fe, and for insight into size distribution measurements and changes over time. Avoids problems with particle aggregation and dissolution between sampling and measurement.

Laboratory analysis			
Mossbauer	>100 mg/L		nZVI only. Lab technique, but can be applied to field samples that are frozen after collection.
H ₂ Acid digestion		< 500 nm	nZVI only. When combined with total Fe measurements, Fe ⁰ /Fe _{tot} ratios can be used to follow reactivity.
Laser diffraction (Mastersizer)	> 500 mg/L	0.6 – 1 µm	Applicable for most particles. FeOx below the limit of detection for size
Time of Transition (EyeTech)	< 500 mg/L	0.6 – 600 µm	Sedimentation problems with nZVI (Nanofer) and milled Fe. FeOx below the limit of detection for size
Dynamic light scattering (Zetasizer)	< 200 mg/l	1 nm - 1 µm	Applicable for most particles. Sedimentation problems with nZVI (Nanofer) and milled Fe.
Carbolron and Zeolites			
Carbolron: Particulate organic carbon	5 mg/L	NR	Filtration of water sample.
Carbolron: C/Fe ratios		NR	Preliminary <i>in situ</i> test
Carbolron: TPO	Ca 0.3 % wt		Sediments. Test on NanoRem porous media
Fe- Zeolites: DLS, Fe-content, laser diffraction	0.1-2.5 g/L		As above
Fe-Zeolites: BET	0,03 % wt		Test on acid washed sand
Fe-Zeolites: target adsorption	0,01 % wt		Test on M:1 (Dorsilit)
NA – Not relevant			

The applicability and feasibility of monitoring tools for Carbo-Iron detection are currently based on off-site lab tests and will be intensified and extended to field applications as soon as the large-scale experiments are conducted. Two tracing methods (Fe/C ratios and TPO) have been developed which successfully proved to detect and distinguish Carbo-Iron from other particle types and background sediment. A series of indirect methods for quantification of the zeolite content in sediments have been tested using standard NanoRem porous media. At present, the target contaminant adsorption appears most suitable with respect to handling and DL.

8 List of References

- Braunschweig, J., et al. "Reevaluation of colorimetric iron determination methods commonly used in geomicrobiology" *Journal of Microbiological Methods*, 2012. 89: 41-48.
- Buhrke, V.E., Jenkins, R., Smith, D.K. Preparation of specimens for X-ray fluorescence and X-ray diffraction analysis. New York: John Wiley & Sons, Inc.; 1998.
- Clearfield, A., Reibenspies, J.H., Bhuvanesh, N. Principles and Applications of Powder Diffraction. Oxford: Blackwell Publishing Ltd; 2008.
- Filip, J., Zboril, R., Schneeweiss, O., Zeman, J., Cernik, M., Kvapil, P., Otyepka, M. Environmental applications of chemically pure natural ferrihydrite. *Environ Sci Technol* 2007;41:4367–4374.
- Filip, J., Karlický, F., Marušák, Z., Černík, M., Otyepka, M. & Zbořil, R. Anaerobic Reaction of Nanoscale Zero-valent Iron with Water: Mechanism and Kinetics. *J Phys Chem C* 2014;118:13817–13825.
- Fu, F., Dionysiou, D.D., Liu, H. The use of zero-valent iron for groundwater remediation and wastewater treatment: A review. *J Haz Mat* 2014;267:194–205.
- Johnson, R-L, Nurmi, J.T., O'Brien, G.S., Fan, D, Reid L., Shi, Z., Salter-Blanc, A.J., Tratnyek, P.G., Lowry, G.V. 2013. Field-scale transport and transformation of carboxymethylcellulose-stabilized nano zero-valent iron, *Environmental Science and Technology*. 47, 1573-1580.
- Lind O.C and Oughton D H (2014) Analytical Toolbox Database, IDL 6.1 NanoRem FP 7 Project GA No 309517. www.nanorem.eu
- Nuyts G., Cagno S., Lind O.C., Oughton D.H., Janssens K. (unpublished results) XAFS profiles of oxidation state ds of Fe compounds.
- Oughton, D.H., Hertel-Aas, T., Pellicer, E., Mendoza, E., Joner, E.J., 2008. Neutron activation of engineered nanoparticles as a tool for tracing their environmental fate and uptake in organisms. *Environmental Toxicology and Chemistry* 27, 1883-1887.
- Sharma, V.K., Klingelhöfer, G., Nishida, T. Mössbauer spectroscopy: applications in chemistry, biology, and nanotechnology. New jersey: John Wiley & Sons, Inc.; 2014.
- Shi, Z., Nurmi, J.T, Tratnyek, P.G. 2011. Effects of nano zero-valent iron on oxidation-reduction potential. *Environmental Science and Technology* 45, 1586-1592.
- Teien, H.C., Garmo, O.A., Atland, A., Salbu, B., 2008. Transformation of iron species in mixing zones and accumulation on fish gills. *Environmental Science & Technology* 42, 1780-1786.
- Watts, MP., Coker,VS, Parry, S., Thomas, R., Kalin, R. and Lloyd, JR. (2015) Effective treatment of alkaline Cr(VI) contaminated leachate using a novel Pd-bionanocatalyst; impact of electron donor and aqueous geochemistry. *Applied Catalysis B: Environmental* doi:10.1016/j.apcatb.2015.01.017
- Watts, MP., Coker,VS, Parry, S. Patrick, RAD., Thomas, R., Kalin, R. and Lloyd JR. (2015) Bionanoparticle treatment of alkaline Cr(VI) leachate and chromite ore processing residue. *Applied Geochemistry* 54 27-42
- Williams, C.E., May, R.P., Guinier, A. Small-Angle Scattering of X-Rays and Neutrons. In: Cahn, R.W., Haasen, P., Kramer, J. editors. *Materials science and technology, a comprehensive treatment*; Vol. 2b: Characterization of materials. Weinheim: WILEY-VCH Verlag GmbH & Co. KGaA; 2005. P. 611–656.

Appendix 1: ICP-MS measurements of Rare Earth Elements in NP Stock Solutions and Site reference samples (pre-injection)

Sample	Fe	La	Ce	Pr	Nd	Sm	Eu	Gd	Tb	Dy	Ho
	mg/l	µg/l	µg/l	µg/l	µg/l	µg/l	µg/l	µg/l	µg/l	µg/l	µg/l
<i>Vegas Large Scale Tank Experiment</i>											
Stock FeOx Tank	4400	28	67	6,3	24	4,5	1,4	4,0	0,60	3,6	0,72
Stock FeOx < 10 kDa	<LD	<LD	<LD	<LD	<LD	<LD	<LD	<LD	<LD	<LD	<LD
Background samples total ^a	0,33-0,87	<0,042	0,056	<LD	<0,039	<0,014	<LD	<LD	<LD	<LD	<LD
Background < 10 kDa	<0,31-0,72	<LD	<LD	<LD	<LD	<LD	<LD	<LD	<LD	<LD	<LD
<i>Spolchemie Field Study – nZVI – Site 1</i>											
Stock nZVI	100000	1000	2000	33	110	26	0,21	14	1,8	13	2,6
Stock nZVI < 10 kDa	990	9,8	19	0,43	1,2	0,23	<0,018	0,26	0,029	0,16	<0,033
129-6m-Ref	0,52	0,47	1,2	0,10	0,40	0,070	0,022	0,067	<0,022	<0,069	<0,033
129-8m-Ref	1,0	0,69	1,7	0,16	0,59	0,11	0,031	0,098	<0,022	0,088	<0,033
129-8m-Ref < 10 kDa	<0,31	0,063	0,21	<0,028	0,046	<0,014	<LD	<0,027	<LD	<LD	<LD
<i>Spolchemie Field Study – FeOx – Site 2</i>											
Stock FeOx	3500	24	56	5,3	20	3,7	1,1	3,6	0,51	3,4	0,58
Stock FeOx < 10 kDa	7	0,32	1,2	0,14	0,69	0,14	0,022	0,18	0,028	0,20	0,058
Reference samples total ^b	17-130	0,53-1,1	1,1-1,9	0,12-0,20	0,49-0,93	0,10- 0,22	0,027-0,059	0,14-0,25	0,026-0,035	0,16-0,27	<0,033-0,094
Reference < 10 kDa	4.3 - 130	<0,042-0,33	0,061-0,31	<0,028-0,056	0,079-0,37	0,045-0,12	<0,018-0,038	0,11-0,15	<0,022-0,040	0,061-0,21	<0,028-0,18
Limit of Detection LD	0,092	0,012	0,015	0,0083	0,012	0,0043	0,0055	0,0080	0,0066	0,021	0,0099
Limit of Quantification LQ	0,31	0,042	0,050	0,028	0,039	0,014	0,018	0,027	0,022	0,069	0,033

a – Tank reference sampling points: K-e3D, K-4iE, K-3gE; b – Spolchemie FeOx site 2: Reference sample wells: AW6A 1, AW6A 2 and AW6A 3

Appendix 1: cont.

Sample	Er	Tm	Yb	Lu
	µg/l	µg/l	µg/l	µg/l
Stock FeOx Tank	1,8	0,28	1,2	0,23
Stock FeOx < 10 kDa	<LD	<LD	<LD	<LD
Background samples total ^a	<LD	<LD	<LD	<LD
Background < 10 kDa	<LD	<LD	<LD	<LD
<i>Spolchemie Field Study – nZVI – Site 1</i>				
Stock nZVI	7,8	1,5	7,1	1,9
Stock nZVI < 10 kDa	0,15	<0,027	0,36	0,029
129-6m-Ref	<0,029	<LD	<LD	<LD
129-8m-Ref	0,043	<LD	<0,15	<LD
129-8m-Ref < 10 kDa	<LD	<LD	<LD	<LD
<i>Spolchemie Field Study – FeOx – Site 2</i>				
Stock FeOx	1,6	0,23	1,8	0,32
Stock FeOx < 10 kDa	0,19	0,036	<0,15	0,062
Reference samples total ^b	0,11-0,45	<0,027 - 0,10	<0,15 - 0,96	<0,025 0,22
Reference < 10 kDa	0,14-0,85	<0,027- 0,17	0,23- 1,7	0,042- 0,38
Limit of Detection LD	0,0088	0,0080	0,045	0,0086
Limit of Quantification LQ	0,029	0,027	0,15	0,029